

FERMILAB-Pub-97/95-T
CERN-TH/97-74
hep-ph/9704347

Electroweak Baryogenesis and Higgs Physics ^a

M. Carena[†] and C.E.M. Wagner[‡]

[†] Fermi National Accelerator Laboratory
P.O. Box 500, Batavia, IL 60510, USA

[‡] Theory Division, CERN
CH-1211 Geneva 23, Switzerland

Abstract

Electroweak Baryogenesis is a particularly attractive theoretical scenario, since it relies on physics which can be tested at present high energy collider facilities. Within the Standard Model, it has been shown that the requirement of preserving the baryon number generated at the weak scale leads to strong bounds on the Higgs mass, which are already inconsistent with the present experimental limits. In the Minimal Supersymmetric extension of the Standard Model, we demonstrate that light stop effects can render the electroweak phase transition sufficiently strongly first order, opening the possibility of electroweak baryogenesis for values of the Higgs mass at the LEP2 reach. The generation of the observed baryon asymmetry also requires small chargino masses and new CP-violating phases associated with the stop and Higgsino mass parameters. We discuss the direct experimental tests of this scenario and other relevant phenomenological issues related to it.

April 1997

^aTo appear in *Perspectives on Higgs Physics II*, ed. G.L. Kane, World Scientific, Singapore

ELECTROWEAK BARYOGENESIS AND HIGGS PHYSICS

M. CARENA

FERMILAB, P.O. Box 500, Batavia, IL 60510, USA

C.E.M. WAGNER

CERN, TH Division, CH-1211 Geneva 23, Switzerland

Electroweak Baryogenesis is a particularly attractive theoretical scenario, since it relies on physics which can be tested at present high energy collider facilities. Within the Standard Model, it has been shown that the requirement of preserving the baryon number generated at the weak scale leads to strong bounds on the Higgs mass, which are already inconsistent with the present experimental limits. In the Minimal Supersymmetric extension of the Standard Model we demonstrate that light stop effects can render the electroweak phase transition sufficiently strongly first order, opening the possibility of electroweak baryogenesis for values of the Higgs mass at the LEP2 reach. The generation of the observed baryon asymmetry also requires small chargino masses and new CP-violating phases associated with the stop and Higgsino mass parameters. We discuss the direct experimental tests of this scenario and other relevant phenomenological issues related to it.

1 INTRODUCTION

One of the fundamental problems of particle physics is to understand the origin of the observed baryon asymmetry of the universe. The mechanism for the generation of baryon number may rely on physics at very high energies, of order of the Planck or Grand Unification scale and hence difficult to test at present high energy colliders. Even in this case, the final result for the baryon asymmetry will always be affected by low energy physics. Indeed, although baryon number is preserved in the Standard Model at the classical level, it is violated through anomalous processes at the quantum level¹. As the Universe cools down, unless specific conditions on the baryon and lepton asymmetries generated at high energies are fulfilled², the anomalous processes will tend to erase the baryon asymmetry generated at high energies. If the baryon asymmetry is completely washed out at temperatures far above the weak scale, the observed baryon number must proceed from physical processes at temperatures close to T_c , at which the electroweak phase transition takes place.

Baryogenesis at the electroweak phase transition is a very attractive alternative since it relies only on physics at the weak scale, and it is hence testable in the near future. In principle, the Standard Model (SM) fulfills all the requirements³ for a successful generation of baryon number⁴. Non-equilibrium

processes occur at the first order electroweak phase transition, baryon number is violated by anomalous processes and CP is violated by explicit phases in the CKM matrix. In order to quantitatively estimate the generated baryon number, one should take into account that the baryon number violating processes are effective also after the electroweak phase transition, and are only suppressed by a Boltzman factor

$$\Gamma \simeq T^4 \exp\left(-\frac{E_{\text{sph}}}{T}\right), \quad (1)$$

where the sphaleron energy, E_{sph} , is equal to the height of the barrier separating two topologically inequivalent vacua⁵. The sphaleron energy is given by

$$E_{\text{sph}}(T) \simeq B \frac{2M_W(T)}{\alpha_w(T)} \quad (2)$$

with $B \simeq \mathcal{O}(2)$ being a slowly varying function of the Higgs quartic coupling, M_W the weak gauge boson mass and α_w the weak gauge coupling. If the phase transition were second order, or very weakly first order, the baryon number violating processes would be approximately in equilibrium and no effective baryon number will survive at $T \lesssim T_c$. Comparing the rate, Eq. (1), with the rate of expansion of the universe one can obtain the condition under which the generated baryon number will be preserved after the electroweak phase transition. This implies a bound on the sphaleron energy, $E_{\text{sph}}(T_c)/T_c \gtrsim 45$ ⁶ or, equivalently,

$$\frac{v(T_c)}{T_c} \gtrsim 1. \quad (3)$$

Since $v(T_c)/T_c$ is inversely proportional to the quartic coupling appearing in the low energy Higgs effective potential, the requirement of preserving the generated baryon asymmetry puts an upper bound on the value of the Higgs mass. The actual bound depends on the particle content of the theory at energies of the order of the weak scale. In the case of the Standard Model, the present experimental bounds on the Higgs mass are already too strong, rendering the electroweak phase transition too weakly first order. Hence, within the Standard Model, the generated baryon asymmetry at the electroweak phase transition cannot be preserved⁶, as perturbative^{7–9} and non-perturbative^{10,11} analyses have shown. It is interesting to notice that, even in the absence of experimental bounds, the requirement of a sufficiently strong first order phase transition leads to bounds on the Higgs mass such that the electroweak breaking minimum would become unstable unless new physics were present at scales of the order of the weak scale^{14–16}. We shall review these bounds below. On

the other hand, CP-violating processes are suppressed by powers of m_f/M_V , where m_f are the light-quark masses and M_V is the mass of the vector bosons. These suppression factors are sufficiently strong to severely restrict the possible baryon number generation^{12,13}. Therefore, if the baryon asymmetry is generated at the electroweak phase transition, it will require the presence of new physics at the electroweak scale.

The most natural extension of the Standard Model, which naturally leads to small values of the Higgs masses is low energy supersymmetry. It is hence highly interesting to test under which conditions baryogenesis is viable within this framework^{18–20}. It was recently shown^{21–24} that the phase transition can be sufficiently strongly first order only in a restricted region of parameter space, which strongly constrains the possible values of the lightest stop mass, of the lightest CP-even Higgs mass (which should be at the reach of LEP2) and of the ratio of vacuum expectation values, $\tan\beta$. These results have been confirmed by explicit sphaleron calculations in the Minimal Supersymmetric Standard Model (MSSM)²⁵.

On the other hand, the Minimal Supersymmetric Standard Model, contains, on top of the CKM matrix phase, additional sources of CP- violation and can account for the observed baryon asymmetry.^b New CP-violating phases can arise from the soft supersymmetry breaking parameters associated with the stop mixing angle. Large values of the mixing angle are, however, strongly restricted in order to preserve a sufficiently strong first order electroweak phase transition^{19–21}. Therefore, an acceptable baryon asymmetry requires a delicate balance between the value of the different mass parameters contributing to the left-right stop mixing, and their associated CP-violating phases. Moreover, the CP-violating currents must originate from the variation of the CP-odd phases appearing in the couplings of stops, charginos and neutralinos to the Higgs particles. This variation would be zero if $\tan\beta$ were a constant, implying that the heavy Higgs doublet can not decouple at scales far above T_c , or equivalently, the CP-odd Higgs mass should not be much larger than M_Z . On the other hand, since the phase transition becomes weaker for lighter CP-odd Higgs bosons, a restricted range for the CP-odd and charged Higgs masses may be obtained from these considerations.

The scenario of Electroweak Baryogenesis (EWB) has crucial implications for Higgs physics and imposes important constraints on the supersymmetry breaking parameters. Most appealing, this scenario makes definite predictions,

^bAn interesting scenario, relying only on the Standard Model phases was recently suggested²⁶. However, since it requires a large mixing between the second and third generation squarks, an analysis of the strength of the first order phase transition will be necessary to decide about its viability.

which may be tested at present or near future colliders.

In section 2 we shall present the improved one-loop finite temperature Higgs effective potential. In section 3 we discuss the Standard Model case, on the light of present experimental constraints on the Higgs mass and the requirement of stability of the physical vacuum. In section 4, we study the strength of the electroweak phase transition within the minimal supersymmetric extension of the standard model, discussing in detail the effect of light stops in expanding the allowed Higgs mass range and analyzing the conditions to avoid color breaking minima. We also discuss the strength of the electroweak phase transition in the cases of large and small values of the CP-odd Higgs mass, and analyse the new sources of CP-violation which may contribute to the generation of baryon asymmetry within the MSSM. In section 5 we study the generation of baryon asymmetry. In section 6 we elaborate on the experimental tests of this scenario both at LEP2 and the Tevatron, and discuss the predictions for some rare flavor changing neutral current processes within this framework. In section 7 we summarize the prospects for electroweak baryogenesis.

2 FINITE TEMPERATURE HIGGS EFFECTIVE POTENTIAL

As we explained above, the requirement of preserving the baryon asymmetry after the phase transition implies that $v(T_c)/T_c$ must be larger than one. To extract the implications of this requirement, a detailed knowledge of the finite temperature effective potential of the Higgs field is needed. The finite temperature effective potential for the neutral component of the Higgs field may be computed at the one-loop level²⁷,

$$V(\phi, T) = V_{\text{tree}}(\phi) + V_1(\phi, 0) + V_1(\phi, T) \quad (4)$$

where $V_{\text{tree}}(\phi)$, $V_1(\phi, 0)$ and $V_1(\phi, T)$ are the tree level, one-loop zero temperature and one-loop finite temperature contributions to the effective potential, respectively. Their expressions are given by

$$\begin{aligned} V_{\text{tree}}(\phi) &= m^2 \phi^2 + \frac{\lambda}{2} \phi^4 \\ V_1(\phi, 0) &= \sum_i \frac{n_i}{64\pi^2} m_i^4(\phi) \left[\log \left(\frac{m_i^2(\phi)}{Q^2} \right) - c_i \right] \\ V_1(\phi, T) &= \sum_i \frac{n_i}{2\pi^2 \beta^4} \int_0^\infty dx x^2 \log \left(1 \pm \exp - (x^2 + \beta^2 m_i^2(\phi))^{1/2} \right), \quad (5) \end{aligned}$$

where $m_i(\phi)$ is the mass of the i -field in the background of the field ϕ , n_i is its total number of degrees of freedom, $c_i = 5/6$ for vector bosons and $3/2$

for scalars and fermions. β^{-1} is proportional to the temperature and the plus and minus sign in $V_1(\phi, T)$ are associated with fermionic and bosonic particles, respectively. Observe that the contribution of heavy particles to the temperature dependent part of the effective potential is exponentially suppressed. For values of the masses $m_i(\phi) \lesssim 2 T$, the effective potential admits a high temperature expansion. In this limit, the contribution of bosonic particles to the Higgs effective potential is given by²⁷

$$V_1^b(\phi, T) = \sum_i n_i \left\{ \frac{m_i^2(\phi)}{24\beta^2} - \frac{1}{12\pi} \frac{m_i^3(\phi)}{\beta} - \frac{1}{64\pi^2} m_i^4(\phi) \log(m_i^2(\phi)\beta^2) + \dots \right\} \quad (6)$$

while that of fermions is given by

$$V_1^f(\phi, T) = \sum_i n_i \left\{ \frac{m_i^2(\phi)}{48\beta^2} + \frac{m_i^4(\phi)}{64\pi^2} \log(m_i^2(\phi)\beta^2) + \dots \right\}. \quad (7)$$

Therefore, in the region of validity of the high temperature expansion, the effective potential reads,

$$V(\phi, T) = D(T^2 - T_0^2)\phi^2 - ET\phi^3 + \frac{\lambda}{2}\phi^4 + \dots \quad (8)$$

where D , E and λ are temperature dependent functions, T_0 is the temperature at which the curvature of the potential vanishes at the origin and we have chosen the normalization such that $\langle \phi \rangle = v/\sqrt{2}$, with $v(0) \sim 246$ GeV. The minimization of the potential at $T = T_c$, the temperature at which the electroweak symmetry breaking and the electroweak symmetry preserving minima become degenerate, leads to

$$\frac{\phi(T_c)}{T_c} = \frac{E}{\lambda}. \quad (9)$$

Hence, the strength of the phase transition is directly proportional to the coefficient of the cubic term induced by the presence of bosonic particles, like the gauge bosons, with masses $m_B = k_B\phi^2$ (see Eq. (6)).

Higher loop corrections are important to define the correct infrared properties of the effective potential, and to reduce its gauge dependence. The most important corrections come from the so-called Daisy graphs⁷, which effectively amount to replace

$$\sum_i \frac{n_i m_i^3(\phi)}{12\pi} \rightarrow \sum_i \frac{n_i m_i^3(\phi, T)}{12\pi} \quad (10)$$

in Eq. (6), where

$$m_i^2(\phi, T) = m_i^2(\phi) + \Pi(T) \quad (11)$$

and $\Pi(T)$ is the temperature dependent vacuum polarization contribution to the thermal masses.

An important observation is that the strength of the phase transition is inversely proportional to the squared of the Higgs mass. This is due to the fact that, at zero temperature

$$m_H^2 = \lambda v^2, \quad (12)$$

and the value of λ at the critical temperature is of the order of its zero temperature value. Hence, from Eqs. (3), (9) and (12), the requirement of preservation of the baryon asymmetry leads to an upper bound on the Higgs mass.

3 THE STANDARD MODEL CASE

3.1 The Electroweak Phase Transition

In the Standard Model, the effect of including thermal masses, Eq. (11), implies that only the transverse modes of the electroweak gauge bosons will contribute to the cubic term in the effective potential and hence the Daisy improvement leads to a weaker phase transition than the one predicted at the one-loop level. The coefficient of the cubic term is given by

$$E_{\text{SM}} = \frac{2}{3} \left(\frac{2M_w^3 + M_Z^3}{\sqrt{2}\pi v^3} \right) \quad (13)$$

and hence the upper bound on the Higgs mass derived from Eqs. (3) and (9) is

$$m_H \lesssim 40 \text{ GeV}. \quad (14)$$

Although the Daisy resummation includes the dominant higher loop corrections to the effective potential, there are additional two-loop effects which have been shown to lead to non-negligible corrections⁸, making the phase transition more strongly first order and increasing slightly the above upper bound on the Higgs mass. Non-perturbative effects have been taken into account through lattice studies¹⁰. These simulations have been done both in four dimensions as in the effective three dimensional theory arising at high temperatures. A more involved perturbative resummation has been performed⁹, showing excellent agreement with the lattice results¹¹. In general, the results for the upper bound on the Higgs mass derived from the non-perturbative studies do not differ in a significant way from those ones coming from perturbative

analyses. Numerically, the upper bound obtained from the lattice is somewhat higher than the results obtained from the improved one-loop analysis. The result of the one-loop analysis, Eq. (14), may be hence quoted as a conservative bound on the Higgs mass.

3.2 Stability Bounds and Experimental Limits on m_H .

The low values of the Higgs mass required to preserve the baryon asymmetry are clearly in conflict with the current experimental bounds on this quantity. The present LEP bound on the Standard Model Higgs mass reads²⁹

$$m_H^{SM \text{ exp.}} \gtrsim 70\text{GeV} \quad (15)$$

and hence, for the mechanism of electroweak baryogenesis to survive, new physics should be present at the weak scale.

Actually, this argument might have been made even in the absence of experimental constraints, by analysing the stability of the physical vacuum^{14–16}. This may be understood by considering the renormalization group improved effective potential for the neutral Higgs at zero temperature, which is approximately given by

$$V(\phi) = m^2\phi^2 + \frac{\lambda(\phi)}{2}\phi^4, \quad (16)$$

where $\lambda(\phi)$ means that the quartic coupling must be evaluated at the relevant scale at which the effective potential is analysed. The dominant contributions to the renormalization group equation of the Higgs quartic coupling are

$$\frac{d\lambda}{dt} = \frac{3}{8\pi^2} (\lambda^2 + \lambda h_t^2 - h_t^4) + \text{electroweak corrections}, \quad (17)$$

where h_t is the top quark Yukawa coupling, $t = \log(Q^2/\Lambda^2)$, with Q the renormalization group scale and Λ the cutoff of the effective theory. For large values of λ , the quartic coupling of the Higgs fields, grows indefinitely with rising energy and an upper bound on m_H follows from the requirement of perturbative consistency of the theory up to a given cutoff scale Λ below M_{Pl} . The upper bound on m_H depends mildly on the top quark mass through the impact of the top quark Yukawa coupling on the running of the quartic coupling λ .

On the other hand, the effect of the large values of h_t on the renormalization group evolution of the quartic coupling, may drive λ to negative values at large energy scales, thus destabilizing the standard electroweak vacuum. The requirement of vacuum stability in the Standard Model imposes a lower bound on the Higgs boson mass for a given cutoff scale. This bound on m_H is defined

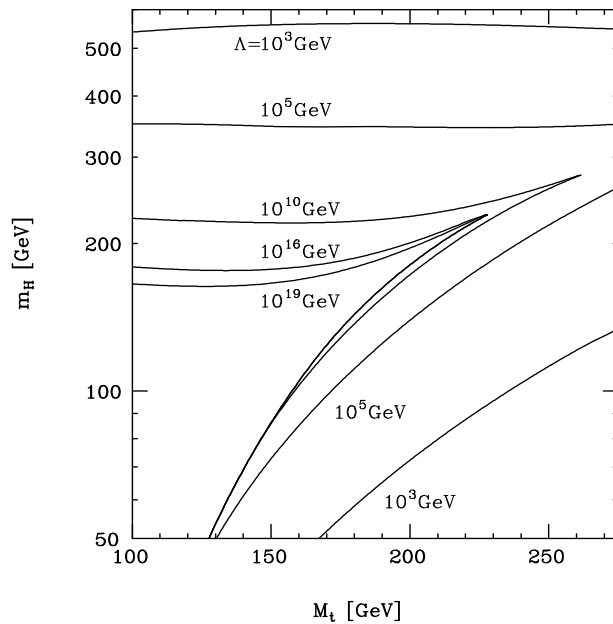


Figure 1: *Bounds on the Higgs mass as a function of the top quark mass for different values of the scale Λ , at which new physics is expected to appear.*

as the lower value of m_H for which $\lambda(\phi) \geq 0$ for any value of ϕ below the scale Λ at which new physics beyond the Standard Model should appear. From Eq. (17), it is clear that the stability condition of the effective potential demands new physics at lower scales for larger values of m_t and lower values of m_H .

Fig. 1²⁸ shows the perturbativity and stability bounds on m_H as a function of the physical top quark mass M_t , for different values of the cutoff Λ at which new physics is expected. Present experimental results lead to a precise knowledge of the value of the top quark mass, $M_t = 175 \pm 6$ GeV¹⁷. Hence, as follows from Fig. 1, independently of the experimental bounds on the Higgs mass, the theoretical upper bound on the Higgs mass obtained from the requirement of preserving the baryon asymmetry, $m_H \simeq 40$ GeV, implies an upper bound on the scale of new physics of the order of the electroweak scale. This new physics will affect the structure of the effective potential at the weak scale, and hence the upper bound on the Higgs mass derived from requiring a

sufficiently strong first order phase transition has to be revised.

4 BEYOND THE STANDARD MODEL: SUPERSYMMETRY

The arguments presented in section 3 depend strongly on the structure of the effective Higgs potential. Hence, the Higgs mass bounds could be simply avoided by complicating the Higgs structure. Models with two Higgs doublets are among the simplest ones, and hence they have attracted some attention. Two Higgs doublet models, in general, lead to charge breaking minima, unless the vacuum expectation values of both Higgs doublets are alligned in such a way that the electromagnetic symmetry is preserved. Moreover, they generally lead to flavor changing neutral currents which are beyond the present experimental limits. There are several ways to avoid these problems, and models of this type have been analysed in the literature. However, there is no clear motivation for the extension of the Higgs sector within the Standard Model. On the contrary, two Higgs doublets are necessary in the context of supersymmetric theories.

The most appealing extension of the Standard Model is the Minimal Supersymmetric Standard Model (MSSM) ³⁰. Supersymmetry relates bosonic and fermionic degrees of freedom. For each chiral fermion (gauge boson) of the Standard Model, a complex scalar (Majorana fermion) appears in the theory, with equal gauge quantum numbers as the Standard Model field ones. Moreover, supersymmetry implies a relation between the couplings of the bosonic and fermionic degrees of freedom, yielding a cancellation of the quadratic divergencies associated with the radiative corrections to the scalar Higgs masses, and providing a technical explanation of the hierarchy stability from M_{Pl} to the electroweak scale.

Supersymmetry provides a solution to most of the problems affecting the multi-Higgs systems. Two Higgs doublets are naturally required, to cancel the anomalies generated by the superpartners of the Higgs bosons. Moreover, flavor changing neutral currents are naturally suppressed since supersymmetry requires that only one of the Higgs doublets couples to the up-like (down-like) quarks. In addition, the effective Higgs potential is such that the vacuum state is naturally alligned towards a charge conserving minimum in the Higgs sector of these models.

The Higgs spectrum of the Minimal Supersymmetric extension of the Standard Model consists of two CP-even bosons, a CP-odd and a charged Higgs bosons ³¹. The heaviest CP-even and the charged Higgs masses are of the order of the CP-odd Higgs mass, m_A , and for large values of m_A they form a heavy Higgs doublet which decouples at low energies. In this limit, the lightest Higgs doublet contains the three Goldstone modes, as well as a CP-

even state. Moreover, supersymmetry relates the Higgs quartic couplings to the weak gauge couplings leading to an upper bound on the lightest CP-even Higgs mass,

$$m_h^2 \leq M_Z^2 \cos^2 2\beta + \text{rad. corr.}, \quad (18)$$

where $\tan \beta = v_2/v_1$ and v_2 (v_1) is the vacuum expectation value of the Higgs field H_2 (H_1) which couples to the up (down) quarks. The last term in the above equation denotes the radiative corrections, which are induced through supersymmetry breaking effects. The main contributions will be discussed in section 4.1.

Supersymmetry is particularly appealing for the scenario of electroweak baryogenesis, since it naturally provides small values of the Higgs mass, and hence tends to give a relatively strong first order phase transition. Moreover, in a supersymmetric theory the negative contributions of the top quark to the renormalization group evolution of the Higgs quartic couplings are compensated by the effects of its supersymmetric partner, providing a natural solution to the vacuum stability problem. However, since supersymmetry is broken in nature, this argument depends strongly on the supersymmetry breaking scale. Indeed the supersymmetry breaking scale may be identified with the scale of new physics (see section 3). Since the particles which couple more strongly to the Higgs are the top quark and its supersymmetric partners, the relevant scale of new physics, in relation to the stability of the Higgs potential, is given by the stop masses. From Fig. 1 we see that in order to preserve the stability of the effective potential, for a Higgs mass of order of the present experimental bound, the lightest stop mass must be of the order of the weak scale.

4.1 Higgs and Stop Masses in the MSSM

The stop masses have an incidence on the Higgs potential which goes beyond the problem of vacuum stability. The stop radiative corrections affect the value of the parameters appearing in the effective potential of the Higgs field in a way which depends on the exact value of the stop masses³². For values of the stop masses close to the top mass, there is an approximate cancellation between the top and stop loop effects and the tree-level relation between m_h and M_Z , Eq. (18), is recovered. For very large values of the stop masses, instead, the tree-level relation is strongly affected by radiative corrections and the effective theory is similar to a non-supersymmetric two Higgs doublet model.

It is interesting to discuss in some detail the properties of the superpartners of the top quark. The left handed and right handed stops are not mass eigenstates, due to the appearance of effective trilinear couplings between the

left- and right-handed stops and the Higgs fields

$$\mathcal{L}_3 = -h_t \left(\epsilon_{ij} A_t H_2^j Q^i U - \mu^* H_1^{*i} Q^i U \right) + h.c., \quad (19)$$

where Q is the scalar top-bottom left-handed doublet and U is the charge conjugate of the right handed scalar top, A_t is a soft supersymmetry breaking mass parameter and μ is the Higgs superpartner (Higgsino) mass term. Once the neutral components of the Higgs doublets acquire vacuum expectation values, a mixing term appears between the left and right handed stops, leading to the following mass matrix

$$\mathcal{M}_{st}^2 = \begin{bmatrix} m_Q^2 + m_t^2 + D_L & m_t (A_t - \mu^* / \tan \beta) \\ m_t (A_t^* - \mu / \tan \beta) & m_U^2 + m_t^2 + D_R \end{bmatrix} \equiv \begin{bmatrix} m_{LL}^2 & m_{LR}^2 \\ m_{LR}^2 & m_{RR}^2 \end{bmatrix}, \quad (20)$$

where m_Q^2 and m_U^2 are the soft supersymmetry breaking square mass parameters of the left and right handed stops, respectively, D_L and D_R are the (relatively small) D-term contributions to the stop masses, and $m_t = h_t < H_2 >$ is the running top quark mass. The stop mass eigenvalues are then given by

$$m_{\tilde{T},i}^2 = \frac{m_{LL}^2 + m_{RR}^2}{2} \pm \sqrt{\left(\frac{m_{LL}^2 - m_{RR}^2}{2} \right)^2 + |m_{LR}^2|^2}. \quad (21)$$

The lightest CP-even Higgs mass is a monotonically increasing function of the CP-odd Higgs mass m_A . As mentioned above, for large values of the CP-odd Higgs mass, $m_A \gg M_Z$, the heavy Higgs doublet decouples and we obtain an upper bound on the lightest CP-even Higgs mass. This value has been computed at the one and two-loop level, and considering a renormalization group resummation³². In the large m_A limit, with $m_Q \simeq m_U$, a simple formula is obtained at the two-loop level³³,

$$\begin{aligned} m_h^2 &= M_Z^2 \cos^2 2\beta \left(1 - \frac{3m_t^2}{4\pi^2 v^2} t \right) \\ &+ \frac{3m_t^4}{2\pi^2 v^2} \left[\frac{X_t}{2} + t + \frac{1}{16\pi^2} \left(\frac{3m_t^2}{v^2} - 32\pi\alpha_3 \right) (X_t t + t^2) \right] \end{aligned} \quad (22)$$

where m_t and $\alpha_3 = g_3^2/4\pi$, with g_3 the strong gauge coupling, are evaluated at the top quark mass scale,

$$t = \log \left(\frac{M_S^2}{m_t^2} \right) \quad X_t = \frac{2|\tilde{A}_t|^2}{M_S^2} \left(1 - \frac{|\tilde{A}_t|^2}{12M_S^2} \right) \quad (23)$$

with $\tilde{A}_t = A_t - \mu^*/\tan\beta$, $M_S^2 = (m_Q^2 + m_U^2)/2 + m_t^2$, and we have implicitly assumed that $|m_t \tilde{A}_t| \lesssim 0.5 M_S^2$.

The first term in Eq. (22) reproduces the tree-level contribution to the lightest Higgs mass, Eq. (18). The tree level value of the lightest Higgs mass increases for larger values of $\tan\beta$ and tends to zero for $\tan\beta$ equal to one. The most important radiative corrections to the Higgs mass value are positive, proportional to m_t^4 , and increase logarithmically with the supersymmetry breaking scale M_S . The stop mixing parameter plays also a very important role in determining the Higgs mass value. A maximum value for the Higgs mass is obtained for $|\tilde{A}_t| \simeq \sqrt{6} M_S$. Such large values of the stop mass mixing parameter are, however, disfavor by model building considerations. As we shall show in section 4.2, large values of $|\tilde{A}_t| \gtrsim 0.5 M_S$ also make the phase transition more weakly first order.

Since the phase transition becomes stronger for lower values of the Higgs mass, it is interesting to analyse the conditions under which the lightest CP-even Higgs mass becomes close to the present experimental bound $m_h \gtrsim 70$ GeV. Low values of the Higgs mass $m_h \lesssim 85$ GeV are only obtained for $\tan\beta \lesssim 4$. Very low values of $\tan\beta$ are associated with large values of the top quark Yukawa coupling, and for a given value of m_t a lower bound on $\tan\beta$ may be obtained by requiring perturbative consistency of the theory up to scales of order of the grand unification scale. This requirement leads to values of $\tan\beta \gtrsim 1.2$ for the acceptable experimental range for the top quark mass⁵⁵. If $\tan\beta$ is close to one, at least one of the stop masses has to be large, in order to overcome the present experimental limits on m_h . For large splittings between the two stop mass eigenvalues, one has to go beyond the approximation of Eq. (22)³³. We shall briefly discuss this case in section 4.2.

4.2 The Electroweak Phase Transition

Lightest stop mass effects on the phase transition.

As we discussed in section 3, for a fixed Higgs mass, the strength of the first order phase transition may be enhanced by increasing the value of the effective cubic term in the finite temperature Higgs potential. This may be achieved by the presence of extra bosonic degrees of freedom³⁴, with sizeable couplings to the Higgs sector. Within the minimal supersymmetric model, the bosonic particles which couple strongly to the Higgs which acquires vacuum expectation value are the supersymmetric partners of the top quark. Since the cubic term is screened by field independent mass contributions, a relevant enhancement of the cubic term of the effective Higgs potential may only be obtained for small values of the lightest stop mass $m_{\tilde{t}} \lesssim m_t$ ²¹.

The lightest stop must be mainly right-handed in order to naturally suppress its contribution to the parameter $\Delta\rho$ and hence preserve a good agreement with the precision measurements at LEP. This can be naturally achieved if the soft supersymmetry breaking mass parameter of the left-handed stop, m_Q , is much larger than M_Z . We shall first discuss the large CP-odd mass limit, $m_A \gg M_Z$. In this case, the heaviest Higgs doublet decouples and the low energy theory contains only one light Higgs boson, ϕ , with similar properties to the Standard Model one,

$$\phi = \cos \beta H_1 + \sin \beta H_2. \quad (24)$$

For moderate left-right stop mixing, from Eq. (20) it follows that the lightest stop mass is then approximately given by

$$m_{\tilde{t}}^2 \simeq m_U^2 + D_R + m_t^2(\phi) \left(1 - \frac{|\tilde{A}_t|^2}{m_Q^2} \right) \quad (25)$$

where $m_t(\phi) = h_t \sin \beta \phi$. Hence, the lightest stop contribution to the finite temperature Higgs potential, necessary to overcome the SM constraints on the Higgs mass, strongly depends on the value of m_U^2 . At finite temperature, however, the field mass receives vacuum polarization contributions which have a strong impact on the size of the induced cubic terms in the effective finite temperature Higgs potential. Indeed,

$$m_{\tilde{t}}^2(\phi, T) = m_{\tilde{t}}^2(\phi, 0) + \Pi_R(T) \quad (26)$$

where $\Pi_R(T) \simeq 4g_3^2 T^2/9 + h_t^2/6[1 + \sin^2 \beta (1 - |\tilde{A}_t|^2/m_Q^2)]T^2$ is the finite temperature self-energy contribution to the right-handed squarks^{21,35}.

The improved one-loop finite temperature effective potential is then given by

$$V_{\text{eff}}^{\text{MSSM}} = m^2(T)\phi^2 - T \left[E_{\text{SM}}\phi^3 + (2N_c) \frac{m_{\tilde{t}}^{3/2}(\phi, T)}{12\pi} \right] + \frac{\lambda(T)}{2}\phi^4 + \dots \quad (27)$$

where $N_c = 3$ is the number of colors, and E_{SM} is the strength of the cubic term in the Standard Model case.

Observe that the heaviest stop leads to a relevant contribution to the zero-temperature effective potential, which can be absorbed into a redefinition of the mass and quartic coupling parameters. Large values of m_Q have the effect

of increasing the value of the Higgs mass. Indeed, for $m_Q^2 \gg m_U^2$ and moderate values of \tilde{A}_t , the lightest Higgs mass expression at the one-loop level reads,

$$m_h^2 = M_Z^2 \cos^2 2\beta + \frac{3m_t^4}{4\pi^2 v^2} \log \left(\frac{m_t^2 m_T^2}{m_t^4} \right) + \mathcal{O} \left(\frac{\tilde{A}_t^2}{m_Q^2} \right) \quad (28)$$

where $m_T^2 \simeq m_Q^2 + m_t^2$ is the heaviest stop square mass^c. Although larger values of m_h are welcome in order to avoid its experimental bound, since they are associated with an increase of the quartic coupling, they necessarily lead to a weakening of the first order phase transition. Therefore, very large values of m_Q , above a few TeV, are disfavored from this point of view. The finite temperature effects of the heaviest stop are, instead, exponentially suppressed.

From Eq. (27) it follows that, in general, as happens with the longitudinal components of the gauge bosons, the lightest stop contribution to the effective potential does not induce a cubic term. This is mainly due to the fact that the effective stop plasma mass squared at $\phi = 0$,

$$(m_t^{\text{eff}})^2 = -\tilde{m}_U^2 + \Pi_R(T) \quad (29)$$

with $\tilde{m}_U^2 \equiv -m_U^2$, is generally positive and of order of T^2 . If the right handed stop plasma mass at $\phi = 0$, Eq. (29), vanished, a large value of the effective cubic term would be obtained. Since $v(T_c)/T_c \simeq \sqrt{2}E/\lambda$, an upper bound on $v(T_c)/T_c$ may be obtained from these considerations, namely

$$\frac{v(T_c)}{T_c} < \left(\frac{v(T_c)}{T_c} \right)_{\text{SM}} + \frac{2 m_t^3 \left(1 - |\tilde{A}_t|^2 / m_Q^2 \right)^{3/2}}{\pi v m_h^2}, \quad (30)$$

where $m_t = \overline{m}_t(m_t)$ is the on-shell running top quark mass in the $\overline{\text{MS}}$ scheme. The first term on the right hand side of Eq. (30) is the SM contribution

$$\left(\frac{v(T_c)}{T_c} \right)_{\text{SM}} \simeq \left(\frac{40}{m_h[\text{GeV}]} \right)^2, \quad (31)$$

and the second term is the contribution that would be obtained through the right handed stops in the limit of a vanishing plasma mass. The upper bound on $v(T_c)/T_c$ is almost an order of magnitude larger than the one obtained in the Standard Model, implying that Higgs masses of order M_Z may be consistent with electroweak baryogenesis. Although the exact cancellation of the effective

^cThe two loop corrections to the Higgs mass, in the limit of $m_Q^2 \gg m_U^2$ are also available³³

stop mass at $\phi = 0$ is not likely to occur, it is clear that a partial cancellation is necessary to increase the cubic term coefficient considerably^d. A small plasma mass can only be obtained through sizeable values of \tilde{m}_U , this means, negative sizeable values of the right-handed stop mass parameter. Moreover, as it is clear from Eq. (25), the trilinear mass term, \tilde{A}_t , must be $|\tilde{A}_t|^2 \ll m_Q^2$ in order to avoid the suppression of the effective coupling of the lightest stop to the Higgs. Negative values of the right handed stop mass parameter open the window for electroweak baryogenesis. However, they may be associated with the appearance of color breaking minima at zero and finite temperature. It is hence important to discuss briefly the constraints on \tilde{m}_U which may be obtained from the requirement of avoiding color breaking minima deeper than the physical one.

4.3 Color Breaking Minima

Let us first analyse the possible existence of color breaking minima in the case of zero stop mixing. In this case, since $m_Q^2 \gg |m_U|^2$ the only fields which may acquire vacuum expectation values are the fields ϕ and U . At zero temperature, the effective potential is given by

$$V_{eff}(\phi, U) = -m_\phi^2 \phi^2 + \frac{\lambda}{2} \phi^4 + m_U^2 U^2 + \frac{\tilde{g}_3^2}{6} U^4 + \tilde{h}_t^2 \sin^2 \beta \phi^2 U^2 \quad (32)$$

where λ is the radiatively corrected quartic coupling of the Higgs field, with its corresponding dependence on the top/stop spectrum through the one loop radiative corrections, $\tilde{g}_3^2/3$ is the radiatively corrected quartic self-coupling of the field U and \tilde{h}_t^2 is the bi-bilinear $\phi - U$ coupling. The latter couplings are well approximated by $\tilde{g}_3 \simeq g_3$ and $\tilde{h}_t \simeq h_t$. The minimization of this potential leads to three extremes, at: **(i)** $\phi = 0, U \neq 0$; **(ii)** $U = 0, \phi \neq 0$ and **(iii)** $\phi \neq 0, U \neq 0$. The corresponding expressions for the vacuum fields are:

$$\begin{aligned} \text{(i)} \quad U &= 0, & \phi^2 &= \frac{m_\phi^2}{\lambda}; \\ \text{(ii)} \quad \phi &= 0, & U^2 &= \frac{3\tilde{m}_U^2}{\tilde{g}_3^2}; \\ \text{(iii)} \quad \phi^2 &= \frac{m_\phi^2 - 3\tilde{m}_U^2 \tilde{h}_t^2 \sin^2 \beta / \tilde{g}_3^2}{\lambda - 3\tilde{h}_t^4 \sin^4 \beta / \tilde{g}_3^2}, & U^2 &= \frac{\tilde{m}_U^2 - m_\phi^2 \tilde{h}_t^2 \sin^2 \beta / \lambda}{\tilde{g}_3^2/3 - \tilde{h}_t^4 \sin^4 \beta / \lambda}. \end{aligned} \quad (33)$$

^dHigher loop corrections are important, making values of $m_U \gtrsim 0$ possible²²

It is easy to show that the branch (iii) is continuously connected with branches (i) and (ii). One can also show that the branch (iii) defines a family of saddle point solutions, the true (local) minima being defined by (i) and (ii). Hence, the requirement of absence of a color breaking minimum deeper than the physical one is given by ²¹

$$\tilde{m}_U \leq \left(\frac{m_h^2 v^2 \tilde{g}_3^2}{12} \right)^{1/4}. \quad (34)$$

For a Higgs mass $m_h \simeq 70$ GeV, the bound on \tilde{m}_U is of order 80 GeV. This must be compared with the characteristic value of $\Pi_R(T) \simeq \mathcal{O}((100\text{GeV})^2)$, implying that even for values of \tilde{m}_U close to the upper bound on this quantity, a non-negligible screening to the effective cubic term contributions will be present.

It can also be shown that, for $m_Q \gg \tilde{m}_U$, the bound \tilde{m}_U derived above, Eq. (34) is sufficient to assure the stability of the physical ground state for all values of \tilde{A}_t such that the experimental limits on the lightest stop mass are preserved. As we shall show quantitatively below, and it is clear from our previous discussion, Eq. (30), large values of \tilde{A}_t induce a large suppression of the potential enhancement in the strength of the first order phase transition through the light top squark, and are hence disfavoured from the point of view of electroweak baryogenesis.

One must also consider the conditions under which the potential may be metastable, but with a lifetime larger than the age of the universe. Even in this case, in general, the constraint

$$-\tilde{m}_U^2 + \Pi_R(T_c) > 0 \quad (35)$$

must be fulfilled. Indeed, if Eq. (35) were not fulfilled, the universe would be driven to a charge and color breaking minimum at $T \geq T_c$ (see Eq.(36) below). A more conservative requirement can be obtained demanding that the critical temperature for the transition to the color breaking minimum, T_c^U , should be below T_c . Due to the strength of the stop coupling to the gluon and squark fields, one should expect the color breaking phase transition to be stronger than the electroweak one.

Let us analyse the finite temperature effective potential for the U field, which is given by ²¹

$$V_U = (-\tilde{m}_U^2 + \gamma_U T^2) U^2 - T E_U U^3 + \frac{\lambda_U}{2} U^4, \quad (36)$$

where

$$\gamma_U \equiv \frac{\Pi_R(T)}{T^2} \simeq \frac{4g_3^2}{9} + \frac{h_t^2}{6} \left[1 + \sin^2 \beta (1 - \tilde{A}_t^2/m_Q^2) \right]; \quad \lambda_U \simeq \frac{g_3^2}{3}$$

$$\begin{aligned}
E_U \simeq & \left[\frac{\sqrt{2}g_3^2}{6\pi} \left(1 + \frac{2}{3\sqrt{3}} \right) \right] \\
& + \left\{ \frac{g_3^3}{12\pi} \left(\frac{5}{3\sqrt{3}} + 1 \right) + \frac{h_t^3 \sin^3 \beta (1 - \tilde{A}_t^2/m_Q^2)^{3/2}}{3\pi} \right\}.
\end{aligned} \tag{37}$$

The contribution to E_U inside the square brackets comes from the transverse gluons, E_U^g , while the one inside the curly brackets comes from the squark and Higgs contributions [Although included in the numerical results, in the above we have not written explicitly the small hypercharge contributions to E_U and γ_U]. We ignore the gluino and left handed squark contributions since they are assumed to be heavy and, hence, their contributions to the finite temperature effective potential is Boltzman suppressed. Observe that we have written the contributions that would be obtained if the field-independent effective thermal mass terms of the squark and Higgs fields were exactly vanishing at the temperature T_c . Although for values of \tilde{m}_U^2 which induce a large cubic term in the Higgs potential, T_c is actually close to the temperature at which these masses vanish, an effective screening is always present. This means that the value of E_U given above is somewhat overestimated.

The difference between T_0^U , the temperature at which $m_t^{\text{eff}}(\phi = 0) = 0$, and T_c^U , is given by

$$T_c^U = \frac{T_0^U}{\sqrt{1 - E_U^2/2\lambda_U\gamma_U}}. \tag{38}$$

In order to assure a transition from the $SU(2)_L \times U(1)_Y$ symmetric minimum to the physical one at $T = T_c$, we should replace the condition (35) by the condition which assures that $T_c^U < T_c$ ²¹,

$$-\tilde{m}_U^2 + \Pi_R(T) > \tilde{m}_U^2 \frac{\epsilon}{1 - \epsilon} \simeq \tilde{m}_U^2 \epsilon, \tag{39}$$

with $\epsilon = E_U^2/2\lambda_U\gamma_U$, a small number. In the following, we shall require the stability condition, Eq. (39), while using the value of E_U given in Eq. (37). We shall also show the result that would be obtained if only the gluon contributions to E_U , E_U^g , would be considered. The difference between both procedures is just a reflection of the uncertainties involved in our analysis.

Strength of the First Order Phase Transition in the Large m_A Limit

Let us first present the results for zero mixing. Fig. 2 shows the order parameter $v(T_c)/T_c$ for the phase transition as a function of the running light stop mass, for $\tan \beta = 2$, $m_Q = 500$ GeV and $M_t = 175$ GeV. These parameters imply

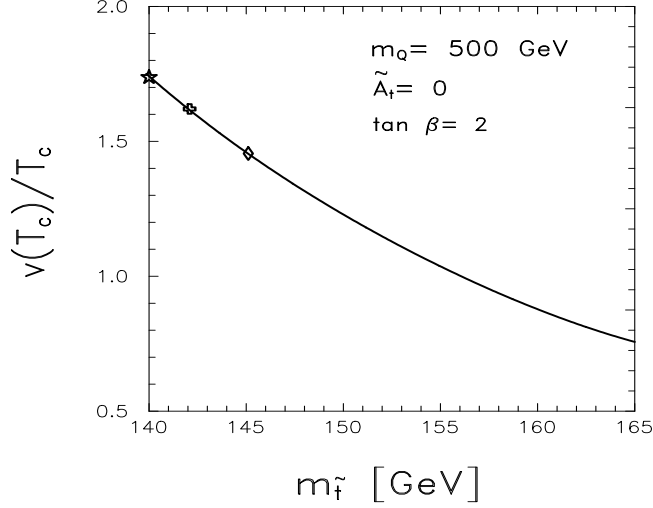


Figure 2: $v(T_c)/T_c$ as a function of $m_{\tilde{t}}$ for $M_t = 175$ GeV, $m_Q = 500$ GeV, $\tilde{A}_t = 0$ and $\tan \beta = 2$. The diamond [cross, star] denotes the value of \tilde{m}_U for which the bound, Eq. (34) is saturated [Eq. (39), while using the total and gluon induced trilinear coefficients, E_U and E_U^g]

a Higgs mass $m_h \simeq 70$ GeV, a result which depends weakly on \tilde{m}_U . We see that for smaller (larger) values of $m_{\tilde{t}}$ (\tilde{m}_U), $v(T_c)/T_c$ increases in accordance with the above discussion in this section. The diamond in fig.2 marks the lower bound on the stop mass coming from the bound on color breaking vacua at $T = 0$, Eq. (34). The cross and the star denote the bounds that would be obtained by requiring the condition (39), while using the total and gluon-induced trilinear coefficient, E_U and E_U^g , respectively. We see that the light stop effect is maximum for values of \tilde{m}_U^2 such that condition (39) is saturated, which leads to values of $m_{\tilde{t}} \simeq 140$ GeV ($\tilde{m}_U \simeq 90$ GeV) and $v(T_c)/T_c \simeq 1.75$. The preservation of condition (34) demands slightly larger stop mass values. The analysis shows that there is a large region of parameter space for which $v(T_c)/T_c \geq 1$ and is not in conflict with any phenomenological constraint.

Fig. 3 shows the results of $v(T_c)/T_c$ for zero mixing and $m_Q = 500$ GeV as a function of $\tan \beta$ and for the values of \tilde{m}_U such that the maximum effect is achieved. We also plot in the figure the corresponding values of the stop and Higgs masses. As in Fig. 2, the solid [dashed] line represents the result when the bound (34) [the stability bound of Eq. (39)] is saturated. We see that $v(T_c)/T_c$ increases for lower values of $\tan \beta$, a change mainly associated

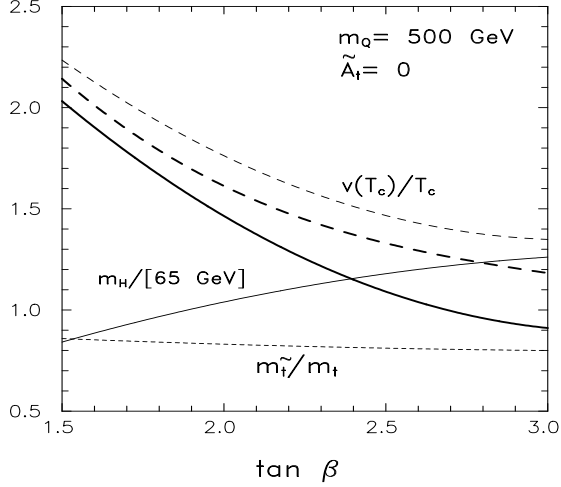


Figure 3: $v(T_c)/T_c$ as a function of $\tan \beta$ for m_Q and \tilde{A}_t as in Fig. 2 and \tilde{m}_U saturating Eq. (34) [solid] and Eq. (39) [thick dashed line when considering the total trilinear coefficient and thin dashed line for the gluon-induced part only]. The additional thin lines are plots of m_h in units of 65 GeV [solid] and \tilde{m}_t/m_t [short-dashed line], corresponding to the values of \tilde{m}_U associated with the solid line.

with the decreasing value of the Higgs mass, or equivalently, of the Higgs self-coupling. For values of $\tan \beta \simeq 2.7$, one gets $v(T_c)/T_c \simeq 1$, and hence the value of the Higgs mass yields the upper bound consistent with electroweak baryogenesis. This bound is approximately given by $m_h \simeq 80$ GeV. If the bound on color breaking minima, Eq. (34), is ignored, then condition (39) yields an upper bound on m_h close to 100 GeV, in accordance with the qualitative discussion presented above (Similar bounds on the Higgs mass, $m_h < 100$ GeV, are obtained when two loops corrections are included and condition (34) is saturated⁵³). Due to the logarithmic dependence of m_h on m_Q , larger values of m_Q have the effect of enhancing the Higgs mass values. It turns out that, for zero mixing, the results for $v(T_c)/T_c$ depend on the Higgs mass and on the value of m_U , but not on the specific value of m_Q . Hence, different values of m_Q have the only effect of shifting (up or down) the preferred values of $\tan \beta$. In particular, the fixed point solution, which corresponds to values of $\tan \beta \simeq 1.6$ for $M_t = 175$ GeV, leads to values of $m_h \gtrsim 70$ GeV and $v(T_c)/T_c \gtrsim 1$, so far m_Q is above 1 TeV and below a few TeV.

The effect of mixing in the stop sector is very important for the present

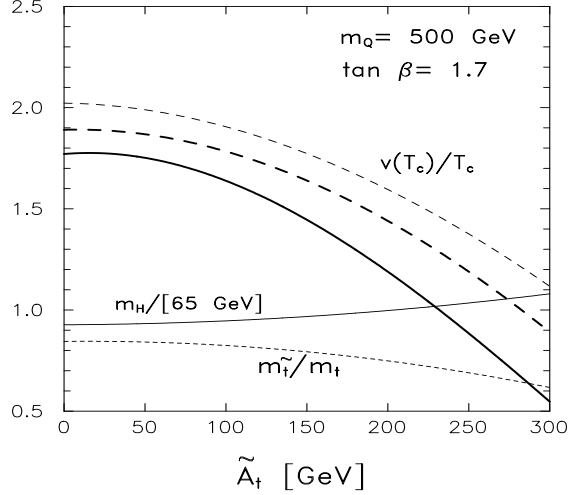


Figure 4: The same as Fig. 3 but as a function on \tilde{A}_t for $\tan \beta = 1.7$

analysis. For fixed values of m_Q and $\tan \beta$, increasing values of \tilde{A}_t have a negative effect on the strength of the first order phase transition for three reasons. First, large values of \tilde{A}_t lead to larger values of the Higgs mass m_h . Second, as shown in Eq. (30) they suppress the stop enhancement of the cubic term. Finally, there is an indirect effect associated with the constraints on the allowed values for \tilde{m}_U . This has to do with the fact that for larger values of \tilde{A}_t , the phase transition temperature increases, making more difficult an effective suppression of the effective mass m_t^{eff} , Eq. (29). Of course, this third reason is absent if the bound (34) is ignored. As we have shown above, for zero mixing the bounds (3), (34) and (39) are only fulfilled for values of the stop mass larger than approximately 140 GeV. Light stops, with masses $m_{\tilde{t}} \lesssim 100$ GeV, can only be consistent with these constraints for larger values of the mixing mass parameter \tilde{A}_t .

Fig. 4 shows the result for $v(T_c)/T_c$ as a function of \tilde{A}_t for $\tan \beta = 1.7$, $m_Q = 500$ GeV, and values of m_U such that the maximal light stop effect is achieved. The same conventions as in Fig. 3 have been used. Due to the constraints on \tilde{m}_U , light stops with $m_{\tilde{t}} \lesssim M_W$, may only be obtained for values of $\tilde{A}_t \gtrsim 0.6 m_Q$. For these values of \tilde{A}_t , the phase transition temperature is large enough to induce large values of m_t^{eff} , for all values of \tilde{m}_U allowed by

Eq. (34). In Fig. 4, we have chosen the parameters such that they lead to the maximum value of the mixing parameter \tilde{A}_t/m_Q consistent with $v(T_c)/T_c \geq 1$ and the Higgs mass bound. For values of \tilde{m}_U such that the bounds on color breaking minima are preserved, the mixing effects on the stop masses are small, and the lightest stop remains heavier than 100 GeV. If, however, the weaker bound, Eq. (39), were required (thin and thick dashed lines in Fig. 4), light stops, with masses of order 80–90 GeV would not be in conflict with electroweak baryogenesis.

Sources of CP-violation and the CP-odd Higgs Mass

The new source of CP-violation, beyond the one contained in the Cabibbo-Kobayashi-Maskawa matrix, may be either explicit³⁶ or spontaneous³⁷ in the Higgs sector (which requires at least two Higgs doublets). In both cases, particle mass matrices acquire a nontrivial space-time dependence when bubbles of the broken phase nucleate and expand during a first-order electroweak phase transition. The crucial observation is that this space-time dependence cannot be rotated away at two adjacent points by the same unitary transformation. This provides sufficiently fast nonequilibrium CP-violating effects inside the wall of a bubble of broken phase expanding in the plasma and may give rise to a nonvanishing baryon asymmetry through the anomalous $(B + L)$ -violating transitions³⁸ when particles diffuse to the exterior of the advancing bubble.

As we already mentioned, new CP-violating phases arise through the soft supersymmetry breaking parameters associated with the left-right stop mixing, namely A_t and μ , Eq. (20). The stop induced current is hence proportional to the variation of the phase of $(A_t H_2 - \mu^* H_1) = |A_t H_2 - \mu^* H_1| \exp(i\phi_{\tilde{A}})$. It is easy to show that

$$\partial_\nu \phi_{\tilde{A}} \sim \text{Im}[A_t \mu] (H_2 \partial_\nu H_1 - H_1 \partial_\nu H_2). \quad (40)$$

The phase of μ enters also in the chargino sector. If we consider the chargino square mass matrix

$$\mathcal{M}_{\text{ch}} \mathcal{M}_{\text{ch}}^\dagger = \begin{bmatrix} M_2^2 + g^2 H_2^2 & g(M_2 H_1 + \mu^* H_2) \\ g(M_2 H_1 + \mu H_2) & |\mu|^2 + g^2 H_1^2 \end{bmatrix}, \quad (41)$$

where $g = 2M_w/v$ is the SU(2) gauge coupling and M_2 is the (assumed) real soft supersymmetry breaking mass of the supersymmetric partners of the weak gauge bosons, the chargino induced CP-violating current is proportional to the variation of the phase of the mixing term, $(M_2 H_1 + \mu^* H_2) = |M_2 H_1 + \mu^* H_2| \exp(i\phi_{\tilde{\mu}})$. It follows that

$$\partial_\nu \phi_{\tilde{\mu}} \sim \text{Im}[M_2 \mu] (H_2 \partial_\nu H_1 - H_1 \partial_\nu H_2). \quad (42)$$

Defining $H^2 = H_1^2 + H_2^2$, to a good approximation, the currents are proportional to the function

$$H_1(z)\partial_z H_2(z) - H_2(z)\partial_z H_1(z) \equiv H^2(z)\partial_z \beta(z), \quad (43)$$

with z the time component of the four vector z_ν . Since the time variation of the Higgs fields in the plasma frame is due to the expansion of the bubble wall through the thermal bath, ignoring the curvature of the bubble wall and assuming that the bubble wall is moving along the z_3 axis with velocity v_w , any quantity becomes a function of $\mathbf{z} = z_3 + v_w z$, the coordinate normal to the wall surface. Eq. (43) should vanish smoothly for values of \mathbf{z} outside the bubble wall. Since $\partial_z \beta \equiv v_w \partial_{\mathbf{z}} \beta$ in Eq. (43) denotes the derivative of the ratio of vacuum expectation values of the Higgs fields, it will be non-vanishing only if the CP-odd Higgs mass takes values of the order of the critical temperature.

Values of the CP-odd Higgs mass $m_A \lesssim 200$ GeV are, however, associated with a weaker first order phase transition. Fig. 5 shows the behaviour of the order parameter v/T in the $[m_A - \tan \beta]$ plane, for $\tilde{A}_t = 0$, $m_Q = 500$ GeV and values of \tilde{m}_U close to its upper bound, Eq. (34). In order to interpret correctly the results of Fig. 5 one should remember that the Higgs mass bounds are somewhat weaker for values of $m_A < 150$ GeV. However, even for values of m_A of order 80 GeV, in the low $\tan \beta$ regime the lower bound on the Higgs mass is of order 60 GeV. Hence, it follows from Fig. 5 that, to obtain a sufficiently strong first order phase transition, $v(T_c)/T_c \gtrsim 1$, the CP-odd Higgs mass must fulfill the condition $m_A \gtrsim 150$ GeV.

In order to compute the CP-violating sources, the variation of the angle β along the bubble wall should be computed. The Higgs profiles along the wall are likely to follow the path of minimal energy connecting the electroweak symmetry preserving and the symmetry breaking vacua in the Higgs potential. The Higgs potential in the case of low values of the CP-odd Higgs mass may be computed by methods similar to those ones explained in section 2, by preserving the field dependence on both Higgs fields^{20,39}. For small values of the fields H_i , as those appearing close to the symmetric phase, the Higgs potential for the neutral CP-even components of the Higgs doublets, H_1 and H_2 , may be approximated by

$$V(H_1, H_2, T) = m_1^2(T)H_1^2 + m_2^2(T)H_2^2 - 2m_3^2(T)H_1H_2 + \mathcal{O}(H_i^3)T + \dots \quad (44)$$

The value of β close to the symmetric phase may be easily computed at the

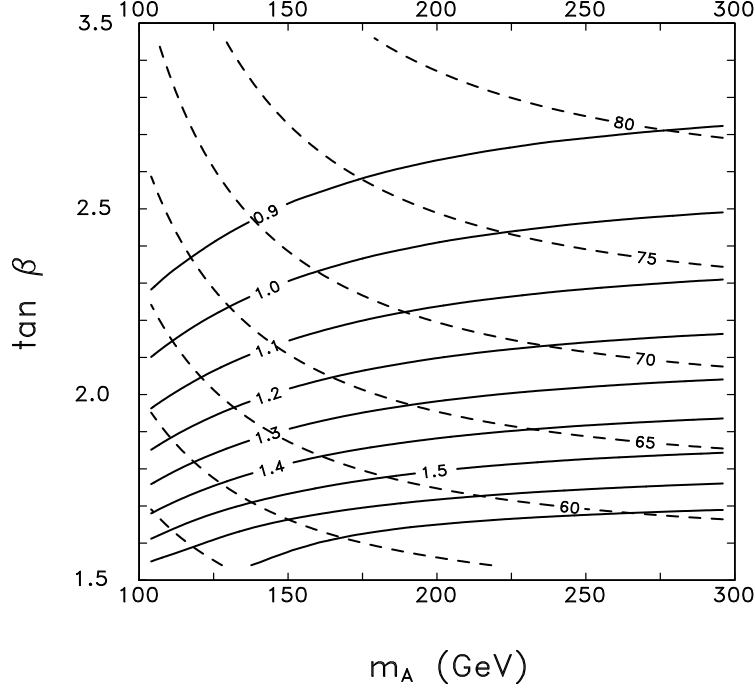


Figure 5: Contour plots of constant values of $v(T_c)/T_c$ (solid lines) and m_h in GeV (dashed lines) in the plane $(m_A, \tan \beta)$. We have fixed $M_t = 175$ GeV and the values of supersymmetric parameters: $m_Q = 500$ GeV, $\tilde{m}_U = \tilde{m}_U^c$ fixed by the charge and color breaking constraint, and $A_t = \mu^* / \tan \beta$.

temperature T_0 at which the curvature at the origin vanishes^e,

$$m_3^4(T_0) = m_1^2(T_0)m_2^2(T_0). \quad (45)$$

Under these conditions, the perturbations of the Higgs fields close to the origin will follow the path such that the value of the potential is minimized along it, namely,

$$m_1^2(T_0)v_1^2 + m_2^2(T_0)v_2^2 - 2m_3^2(T_0)v_1v_2 = 0 \quad (46)$$

or, equivalently,

$$\tan^2 \beta(T_0, H_1 \simeq 0, H_2 \simeq 0) = \frac{m_1^2(T_0)}{m_2^2(T_0)} \simeq \frac{m_1^2(T_c)}{m_2^2(T_c)}. \quad (47)$$

^eStrictly speaking, we are interested in the behaviour of the potential at $T = T_c$. Given the small quantitative difference between T_0 and T_c , we shall identify both temperatures in the following discussion

The exact value of β at the critical temperature may be computed by a numerical simulation of the full effective potential. Hence, the variation of β along the bubble wall may be approximately given by

$$\Delta\beta \simeq \beta(T_c) - \arctan(m_1(T_c)/m_2(T_c)). \quad (48)$$

This quantity tends to zero for large values of m_A like $\Delta\beta \sim H^2/m_A^2$. A numerical estimate³⁹ gives that, for $m_A = 200$ GeV, $\Delta\beta \simeq 0.015$ and hence values of $m_A > 300$ GeV imply a strong suppression of the generated CP-violating sources. We shall fix $m_A = 200$ GeV for most of the following analysis.

5 GENERATION OF THE BARYON ASYMMETRY

Baryogenesis is fueled by CP-violating sources which are locally induced by the passage of the wall^{40,41}. These sources do not provide net baryon number. Indeed, in the absence of baryon number violating processes, the generated baryon number will be zero. Since the CP-violation sources are non-zero only inside the wall, it was first thought that a detail analysis of the rate of anomalous processes inside the bubble wall was necessary to estimate the generated baryon number. However, these first analyses ignored the crucial role played by diffusion⁴³. Indeed, transport effects allow CP-violating charges to efficiently diffuse into the symmetric phase –in front of the advancing bubble wall– where anomalous electroweak baryon number violating processes are unsuppressed. This amounts to greatly enhancing the final baryon asymmetry.

In order to estimate the generated baryon number, a set of coupled classical Boltzmann equations describing particle distribution densities should be solved. These equations take into account particle number changing reactions⁴² and they allow to trace the crucial role played by diffusion⁴³. Since the weak anomalous processes affect only the left handed quarks and leptons, the relevant CP-violating sources are those which can lead through particle interactions to a net chiral charge for the Standard Model quarks. The new CP-violating sources we are considering are associated with the parameters A_t and μ , therefore, the relevant currents are the stop, chargino and neutralino ones. Although the masses of the first and second generation squarks, as well as the sbottom ones, are affected by the phase of the μ parameter, they couple very weakly to the Higgs and hence they play no role in the computation of the CP-violating currents.

The CP-violating sources for left- and right-handed squarks, charginos and neutralinos are converted into sources of chiral quarks via supergauge and top quark Yukawa interactions, respectively. Indeed, the top Yukawa coupling is sufficiently strong, so that the top Yukawa induced processes are

in approximate thermal equilibrium. The same happens with the supergauge interactions, if the gauginos are not much heavier than the critical temperature. Moreover, the strong sphaleron processes are the most relevant sources of first and second generation chiral quarks, and hence they must be taken into account while computing the generated baryon number.

The stop, chargino and neutralino currents at finite temperature may be computed by using diagrammatic methods^{44–46}. For small values of the mixing mass parameter, $|A_t|/m_Q < 0.5$, and large values of $m_Q \gg T$, the CP-violating stop induced current is naturally suppressed. The current associated with neutral and charged higgsinos is the most relevant one, and it may be written as³⁹

$$J_{\tilde{H}}^\mu = \bar{\psi} \gamma^\mu \psi \quad (49)$$

where ψ is the Dirac spinor

$$\psi = \begin{pmatrix} \tilde{H}_2 \\ \tilde{H}_1 \end{pmatrix} \quad (50)$$

and $\tilde{H}_2 = \tilde{H}_2^0$ (\tilde{H}_2^+), $\tilde{H}_1 = \tilde{H}_1^0$ (\tilde{H}_1^-) for neutral (charged) higgsinos.

The vacuum expectation value of the (zero component of the) higgsino current is approximately given by^f

$$\langle J_{\tilde{H}}^0(z) \rangle \simeq \text{Im}(\mu) (H_1(z) \partial_z H_2(z) - H_2(z) \partial_z H_1(z)) \left[3M_2 g^2 \mathcal{G}_{\tilde{H}}^{\tilde{W}} \right], \quad (51)$$

where

$$\mathcal{G}_{\tilde{H}}^{\tilde{W}} \simeq \int_0^\infty dk \frac{k^2}{2\pi^2 \Gamma_{\tilde{H}} \omega_{\tilde{H}} \omega_{\tilde{W}}} \left(\text{Im}(n_{\tilde{H}}) + \text{Im}(n_{\tilde{W}}) \right) I_2(\omega_{\tilde{H}}, \Gamma_{\tilde{H}}, \omega_{\tilde{W}}, \Gamma_{\tilde{W}}) \quad (52)$$

with $n_{\tilde{H}(\tilde{W})} = 1 / \left[\exp \left(\omega_{\tilde{H}(\tilde{W})} / T + i \Gamma_{\tilde{H}(\tilde{W})} / T \right) + 1 \right]$, where $\omega_{\tilde{H}}^2 = k^2 + |\mu|^2$, $\omega_{\tilde{W}}^2 = k^2 + M_2^2$, while $\Gamma_{\tilde{H}}$ and $\Gamma_{\tilde{W}}$ are the damping rate of charged and neutral Higgsinos and winos, respectively. Since these damping rates are dominated by weak interactions^{48,49}, we shall take $\Gamma_{\tilde{H}} \simeq \Gamma_{\tilde{W}}$ to be of order of $5 \times 10^{-2} T$. Moreover, the function I_2 is given by³⁹

$$I_2(a, b, c, d) = \frac{r_1^2 - 1}{2(r_1^2 + 1)[(a+c)^2 + (b+d)^2]} + \frac{r_2^2 - 1}{2(r_2^2 + 1)[(a-c)^2 + (b+d)^2]}, \quad (53)$$

^f We display here only the dominant contribution to the current³⁹

where $r_1 = (a + c)/(b + d)$ and $r_2 = (a - c)/(b + d)$. The above expression, Eq. (51), proceeds from an expansion in derivatives of the Higgs field and it is valid only when the mean free path $\Gamma_{\tilde{W}(\tilde{H})}^{-1}$ is smaller than the scale of variation of the Higgs background determined by the wall thickness and the wall velocity, $\Gamma_{\tilde{W}(\tilde{H})} L_w / v_w \gg 1$.

As mentioned before, the above currents may be used to compute the particle densities, once diffusion and particle changing interaction effects are taken into account. We shall not discuss this in detail here, but we shall limit ourselves to present the most important aspects related to the generation of baryon number.

The particle densities we need to include are the left-handed top doublet $q_L \equiv (t_L + b_L)$, the right-handed top quark t_R , the Higgs particle $h \equiv (H_1^0, H_2^0, H_1^-, H_2^+)$, and the superpartners \tilde{q}_L , \tilde{t}_R and \tilde{h} . The interactions able to change the particle numbers are the top Yukawa interaction with rate Γ_t , the top quark mass interaction with rate Γ_m , the Higgs self-interactions in the broken phase with rate $\Gamma_{\mathcal{H}}$, the strong sphaleron interactions with rate Γ_{ss} , the weak anomalous interactions with rate Γ_{ws} and the gauge interactions. The system may be described by the densities $\mathcal{Q} = q_L + \tilde{q}_L$, $\mathcal{T} = t_R + \tilde{t}_R$ and $\mathcal{H} = h + \tilde{h}$. CP-violating interactions with the advancing bubble wall produce source terms $\gamma_{\tilde{H}} = \partial_z \langle J_{\tilde{H}}^0(z) \rangle$ for Higgsinos and $\gamma_R = \partial_z \langle J_R^0(z) \rangle$ for right-handed stops, which tend to push the system out of equilibrium.

If the system is near thermal equilibrium and particles interact weakly, the particle number densities n_i may be expressed as $n_i = k_i \mu_i T^2 / 6$, where μ_i is the local chemical potential and k_i are statistical factors of order 2 (1) for light bosons (fermions) in thermal equilibrium, and Boltzmann suppressed for particles heavier than T . Assuming that the rates Γ_t and Γ_{ss} are fast so that $\mathcal{Q}/k_q - \mathcal{H}/k_{\mathcal{H}} - \mathcal{T}/k_{\mathcal{T}} = \mathcal{O}(1/\Gamma_t)$ and $2\mathcal{Q}/k_q - \mathcal{T}/k_{\mathcal{T}} + 9(\mathcal{Q} + \mathcal{T})/k_b = \mathcal{O}(1/\Gamma_{ss})$, one can find the equation governing the Higgs density⁴⁷

$$v_\omega \mathcal{H}' - \overline{D} \mathcal{H}'' + \overline{\Gamma} \mathcal{H} - \tilde{\gamma} = 0, \quad (54)$$

where the derivatives are now with respect to \mathbf{z} , \overline{D} is the effective diffusion constant, $\tilde{\gamma}$ is an effective source term in the frame of the bubble wall and $\overline{\Gamma}$ is the effective decay constant. An analytical solution to Eq. (54) satisfying the boundary conditions $\mathcal{H}(\pm\infty) = 0$ may be found in the symmetric phase (defined by $\mathbf{z} < 0$) using a \mathbf{z} -independent effective diffusion constant and a step function for the effective decay rate $\overline{\Gamma} = \tilde{\Gamma}\theta(\mathbf{z})$. A more realistic form of $\overline{\Gamma}$ would interpolate smoothly between the symmetric and the broken phase values. We have checked, however, that the result is insensitive to the specific position of the step function inside the bubble wall.

The analytical solution to the diffusion equations for $\mathbf{z} < 0$ leads to^{39,47}

$$\mathcal{H}(\mathbf{z}) = \mathcal{A} e^{\mathbf{z} v_\omega / \overline{D}}, \quad (55)$$

and for $\mathbf{z} > 0$,

$$\begin{aligned} \mathcal{H}(\mathbf{z}) &= \left(\mathcal{B}_+ - \frac{1}{\overline{D}(\lambda_+ - \lambda_-)} \int_0^{\mathbf{z}} du \tilde{\gamma}(u) e^{-\lambda_+ u} \right) e^{\lambda_+ \mathbf{z}} \\ &+ \left(\mathcal{B}_- - \frac{1}{\overline{D}(\lambda_- - \lambda_+)} \int_0^{\mathbf{z}} du \tilde{\gamma}(u) e^{-\lambda_- u} \right) e^{\lambda_- \mathbf{z}}. \end{aligned} \quad (56)$$

where

$$\lambda_\pm = \frac{v_\omega \pm \sqrt{v_\omega^2 + 4\tilde{\Gamma}\overline{D}}}{2\overline{D}}, \quad (57)$$

and $\tilde{\gamma}(\mathbf{z}) = v_\omega \partial_{\mathbf{z}} J_0(\mathbf{z}) f(k_i)$, J_0 being the total CP-violating current resulting from the sum of the right-handed stop and Higgsino contributions and $f(k_i)$ a coefficient depending on the number of degrees of freedom present in the thermal bath and related to the definition of the effective source⁴⁷. Imposing the continuity of \mathcal{H} and \mathcal{H}' at the boundaries, we find³⁹

$$\mathcal{A} = \mathcal{B}_+ \left(1 - \frac{\lambda_-}{\lambda_+} \right) = \mathcal{B}_- \left(\frac{\lambda_+}{\lambda_-} - 1 \right) = \frac{1}{\overline{D} \lambda_+} \int_0^\infty du \tilde{\gamma}(u) e^{-\lambda_+ u}. \quad (58)$$

From the form of the above equations one can see that CP-violating densities diffuse in a time $t \sim \overline{D}/v_\omega^2$ and the assumptions leading to the analytical form of $\mathcal{H}(\mathbf{z})$ are valid provided $\Gamma_t, \Gamma_{ss} \gg v_\omega^2/\overline{D}$.

The equation governing the baryon asymmetry n_B is given by⁴⁷

$$D_q n_B'' - v_\omega n_B' - \theta(-\mathbf{z}) n_f \Gamma_{ws} n_L = 0, \quad (59)$$

where $\Gamma_{ws} = 6\kappa\alpha_w^4 T$ is the weak sphaleron rate ($\kappa \simeq 1$)⁹, and n_L is the total number density of left-handed weak doublet fermions, $n_f = 3$ is the number of families and we have assumed that the baryon asymmetry gets produced only in the symmetric phase. Expressing $n_L(\mathbf{z})$ in terms of the Higgs number density⁴⁷

$$n_L = \frac{9k_q k_{\mathcal{T}} - 8k_b k_{\mathcal{T}} - 5k_b k_q}{k_{\mathcal{H}}(k_b + 9k_q + 9k_{\mathcal{T}})} \mathcal{H} \quad (60)$$

and making use of Eqs. (55)-(59), we find that

$$\frac{n_B}{s} = -g(k_i) \frac{\mathcal{A} \overline{D} \Gamma_{ws}}{v_\omega^2 s}, \quad (61)$$

⁹The value of κ is still subject of debate^{50,51}

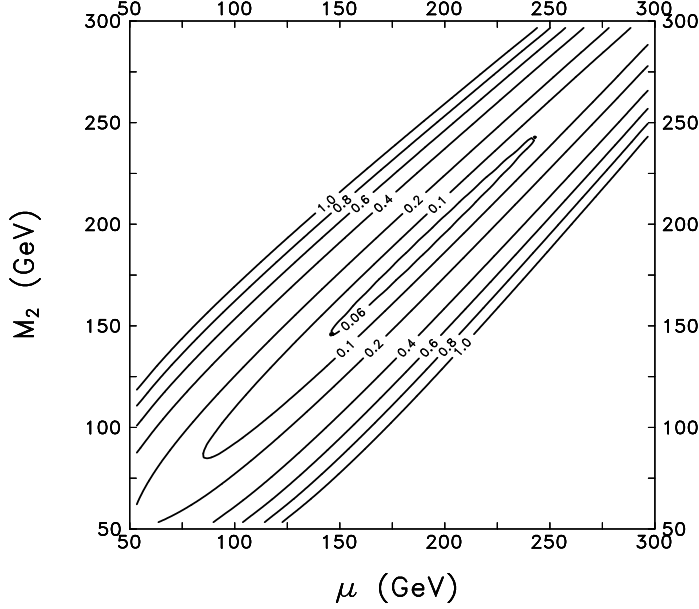


Figure 6: Contour plot of $|\sin \phi_\mu|$ in the plane (μ, M_2) for fixed $n_B/s = 4 \times 10^{-11}$ and $v_\omega = 0.1$, $L_\omega = 25/T$, $m_Q = 500$ GeV, $m_U = m_U^{\text{crit}}$, $\tan \beta = 2$ and $A_t = \mu^* / \tan \beta$.

where $s = 2\pi^2 g_{*s} T^3 / 45$ is the entropy density (g_{*s} being the effective number of relativistic degrees of freedom) and $g(k_i)$ is a numerical coefficient depending upon the light degrees of freedom present in the thermal bath.

Fig. 6 shows the value of the phase of the parameter μ needed to obtain the observed baryon asymmetry, $n_B/s \simeq 4 \times 10^{-11}$, within the approximations given above and using a semirealistic approximation for the Higgs profiles³⁹. The wall velocity is taken to be $v_\omega = 0.1$, while the bubble wall width is taken to be $L_\omega = 25/T$. Our results, are, however, quite insensitive to the specific choice of v_ω and L_ω . It is interesting to note that realistic values of the baryon asymmetry may only be obtained for values of the CP-violating phases of order one, and for a very specific region of the $[\mu - M_2]$ plane. Values of the phases lower than 0.1 are only consistent with the observed baryon asymmetry for values of $|\mu|$ of order of the gaugino mass parameters. This is due to a resonant behaviour of the induced Higgsino current for $|\mu| \simeq M_2$ (See Eq. (51)).

In conclusion, the requirement of a sufficiently strong first order phase transition and of sizeable CP-violating currents may be only satisfied within a very specific region of parameters within the MSSM. The realization of this scenario will imply very specific signatures which may be tested in future runs

of existing experimental facilities. We shall expand on this issue in the next section.

6 EXPERIMENTAL TESTS OF ELECTROWEAK BARYOGENESIS

In the previous sections, we have shown that the scenario of electroweak baryogenesis favors Higgs masses $m_h \lesssim 80$ GeV. Slightly heavier Higgs bosons may be consistent with this scenario only if higher-order (or non-perturbative) effects render the phase transition more strongly first order than what is suggested by one-loop analyses. A hint in this direction was obtained in recent works^{22,52}, where it was shown that, when two-loop corrections are included, the requirement of preservation of the generated baryon asymmetry may be fulfilled, for values of the Higgs masses of order 80 GeV even for $m_U \simeq 0$ (see, for comparison, the results of Fig. 2, for which $m_h \simeq 70$ GeV). An ongoing two-loop analysis for $m_U^2 \lesssim 0$ shows an interesting extension of the allowed m_h region⁵³. As we discussed above, the phase transition may also become moderately stronger assuming that the physical ground state is metastable. In view of all present studies, it may be concluded that a Higgs mass above 95 GeV will put very strong constraints on the scenario of electroweak baryogenesis within the MSSM. Hence, the most direct experimental way of testing this scenario is through the search for the Higgs boson at LEP2.

At LEP2, the lightest CP-even neutral Higgs bosons may be produced in association with Z via Higgs-strahlung

$$e^+e^- \rightarrow Z^* \rightarrow Z h, \quad (62)$$

or in association with the neutral CP-odd Higgs scalar,

$$e^+e^- \rightarrow Z^* \rightarrow h A. \quad (63)$$

The associated Ah production becomes increasingly important for rising values of $\tan\beta$. However, for values of the CP-odd Higgs mass above 100 GeV it is kinematically forbidden, and hence, it is not relevant for testing the scenario of electroweak baryogenesis, for which $m_A \gtrsim 150$ GeV.

The Higgs production rate (62) is equal to the Standard Model one times a projection factor. This projection factor, takes into account the component of the lightest CP-even Higgs on the Higgs which acquires vacuum expectation value (which is the one which couples to the Z in the standard way),

$$\sigma_{MSSM}(e^+e^- \rightarrow Z h) = \sigma_{SM}(e^+e^- \rightarrow Z h) \times \sin^2(\beta - \alpha). \quad (64)$$

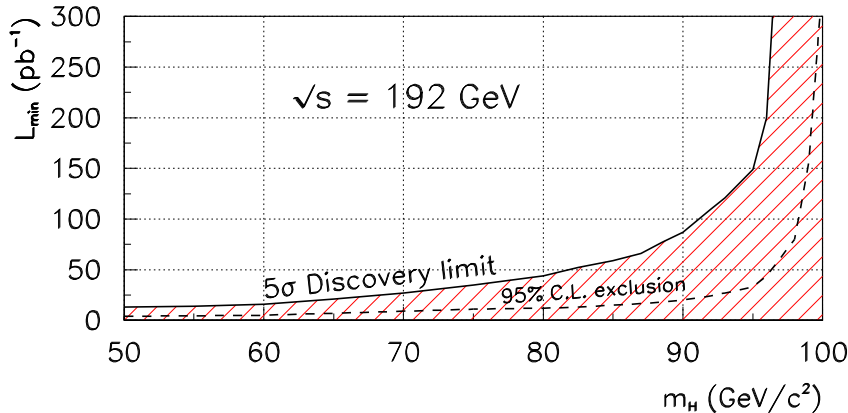


Figure 7: Minimum luminosity needed per experiment, in pb^{-1} , for the combined 5σ discovery (full line) or the combined 95% C.L. exclusion (dashed line) of the Higgs boson as a function of its mass, at a centre-of-mass energy of $\sqrt{s} = 192 \text{ GeV}$.

For large values of the CP-odd Higgs mass, the heavy Higgs doublet decouples and $\sin(\beta - \alpha) \rightarrow 1$. Indeed, the Higgs sector of the theory behaves effectively as the Standard Model one. This transition is achieved rather fast, and for CP-odd Higgs masses above 150 GeV, the cross section differs only slightly from the Standard Model one. Hence, in the limit of interest for this discussion, the mass reach for the lightest CP-even Higgs boson within the MSSM is almost indistinguishable from the one of the Standard Model Higgs.

The search for the Higgs boson is performed by taking into account the dominant decay modes of the Higgs into bottom and τ pairs. Barring the possibility of supersymmetric decay channels, which only appear in very limited regions of parameter space, which will be directly tested through SUSY particle searches, the Higgs decays approximately 90 % of the time into $b\bar{b}$ pairs and 8 % of the time into $\tau\bar{\tau}$ pairs. The Z boson may decay in jets (70 %), charged leptons (10 %) or neutrinos (20 %).

Based on the experimental simulations²⁸, it is possible to derive the exclusion and discovery limits for the lightest CP-even Higgs mass as a function of the luminosity for the expected LEP2 energy range^h. The contours are defined at 5σ for the discovery and 95% C.L. for the exclusion limits. The

^hAs explained above, we are considering scenarios with relatively heavy CP-odd Higgs bosons, for which the limits for the lightest CP-even Higgs coincide with the ones for the SM Higgs

Table 1: *Maximal Higgs masses that can be excluded or discovered with an integrated luminosity L_{min} per experiment at the three representative energy values of 175, 192 and 205 GeV, if the four LEP experiments are combined.*

\sqrt{s} [GeV]	m_H [GeV]	Exclusion L_{min} [pb $^{-1}$] per experiment	m_H [GeV]	Discovery L_{min} [pb $^{-1}$] per experiment
175	83	75	82	150
192	98	150	95	150
205	112	200	108	300

results of the combination of the four experiments for a center of mass energy of $\sqrt{s} = 192$ GeV are shown in Fig. 7. In Table 1 we summarize the minimum luminosities which are needed per experiment for exclusion and discovery for the largest Higgs mass values that can be realistically reached at center-of-mass energies of 175, 192 and 205 GeV; beyond these maximum mass values the required luminosities increase sharply for the exclusion and discovery of the Higgs particle.

It is important to compare the above results with the currently expected energy range and luminosity of the LEP2 experiment. LEP2 is expected to run at a center of mass energy of $\sqrt{s} \simeq 184$ GeV during the summer of 1997 and to collect a total integrated luminosity of approximately 100 pb $^{-1}$ per experiment. Taken into account the results of the above analysis, LEP2 at $\sqrt{s} \simeq 184$ GeV will be able to discover a Standard Model-like Higgs boson with a mass up to approximately 85 GeV. In case of negative searches, this will set a lower bound on the lightest CP-even Higgs mass of order 90 GeV for values of $m_A > 150$ GeV. Clearly, the exact range will finally depend on the real performance of the experiments.

Therefore, if the scenario of electroweak baryogenesis is realized in nature, the 1997 run of the LEP2 experiment has excellent prospects for detecting a Higgs. If, however, no signal is found, this will pose very strong constraints

on the present scenario. For instance, in order to preserve a sufficiently strong first order phase transition the model will be driven into a corner of $\tilde{A}_t \ll m_Q$. In addition, the enhancement of the phase transition due to higher order effects will be crucial. It is clear that non-perturbative information, as well as a deeper insight on the question of metastability of the physical vacuum will then be necessary to decide the fate of this scenario.

Moreover, the LEP2 experiment is expected to achieve a final center of mass energy of about $\sqrt{s} \simeq 192$ GeV and to collect a total integrated luminosity $L \gtrsim 100 \text{ pb}^{-1}$ per year and per experiment. As can be inferred from Table 1, this will lead to a discovery limit of order 95 GeV and an exclusion limit of about 100 GeV. This will definitely test the possibility of baryogenesis at the electroweak scale within the MSSM, since larger values of the Higgs mass are unlikely to be consistent with this scenario.

If the Higgs is found at LEP2, the second test will come from the search for the lightest stop at the Tevatron collider (the stop mass is typically too large for this particle to be seen at LEP). The stop can be pair produced at the Tevatron through gluon processes. It can subsequently decay into bottom and chargino with almost one hundred percent branching ratio, unless the chargino mass is very close or above the stop mass. If this is the case, the stops decays through a loop into charm and neutralino. The signal from the tree level decay can be either a single lepton plus missing energy and b- and light quark-jets, or dilepton plus missing energy and b-jetsⁱ,

$$\begin{aligned} \tilde{t} &\rightarrow b\tilde{\chi}^\pm & \tilde{\chi}^\pm &\rightarrow \tilde{\chi}_1^0 l^\pm \nu & \tilde{\chi}^\pm &\rightarrow \tilde{\chi}_1^0 qq \\ \tilde{t} &\rightarrow b\tilde{\chi}^\pm & \tilde{\chi}^\pm &\rightarrow \tilde{\chi}_1^0 l^\pm \nu & \tilde{\chi}^\pm &\rightarrow \tilde{\chi}_1^0 l^\pm \nu. \end{aligned} \quad (65)$$

If the above channel is kinematically forbidden, the stop signal will then be missing energy plus two acollinear jets,

$$\tilde{t} \rightarrow c\tilde{\chi}_1^0. \quad (66)$$

At present, the D0 experiment has analysed only 14 pb^{-1} of the 100 pb^{-1} data in the $\tilde{t} \rightarrow \tilde{\chi}_1^0 c$ channel and they are able to search for stop masses up to about 100 GeV, depending on the values of the neutralino mass considered. Studies about the prospects for stop searches at the Run II of the Tevatron⁵⁶ (main injector phase at 2 TeV center of mass energy and 2 fb^{-1} of integrated luminosity) show a maximal mass reach for stops of about 150 GeV in the $\tilde{t} \rightarrow \tilde{\chi}_1^\pm b$ channel and about 120 GeV in the $\tilde{t} \rightarrow \tilde{\chi}_1^0 c$ channel. Forseen upgrades of the Tevatron achieving a total integrated luminosity of $10/25 \text{ fb}^{-1}$ will allow

ⁱwe are only considering the case of exact R-Parity conservation

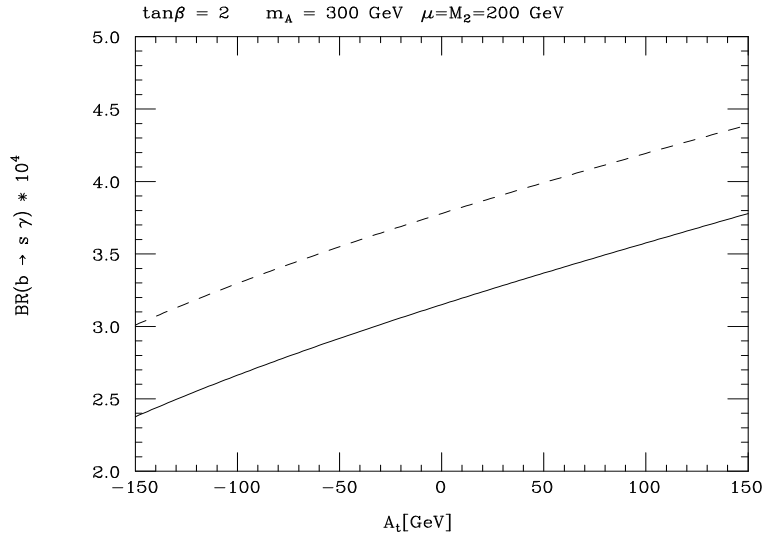


Figure 8: $\text{BR}(b \rightarrow s\gamma)$ as a function of A_t , for $\mu = M_2 = 200$ GeV, $m_A = 300$ GeV, $\tan\beta = 2$, $M_t = 175$ GeV, $m_Q = 500$ GeV, $m_U = m_U^{\text{crit}}$ (fixed by the charge and color breaking constraint), and the first and second generation squark masses equal to 1 TeV.

to discover a top squark with mass below the top quark, although optimization in the event selection procedure is necessary, specially in the neutralino-charm decay channel. Hence, already the Run II of the Tevatron to begin in 1999, will start testing an important region of the stop mass range consistent with electroweak baryogenesis. The foreseen upgrades, if approved, will provide a crucial test of the framework under analysis.

If both particles are found, the last crucial test will come from B physics. The selected parameter space leads to values of the branching ratio $\text{BR}(b \rightarrow s\gamma)$ different from the Standard Model case⁵⁷. Although the exact value of this branching ratio depends strongly on the value of m_A and the μ and A_t parameters, the typical difference with respect to the Standard Model prediction is of the order of the present experimental sensitivity and hence in principle testable in the near future. Indeed, for the typical spectrum considered here, due to the relatively low values of the light charged Higgs mass, the branching ratio $\text{BR}(b \rightarrow s\gamma)$ is somewhat higher than in the SM case, unless it is properly cancelled by the light stop contributions. Figure 8 shows the dependence of $\text{BR}(b \rightarrow s\gamma)$ on A_t for $M_2 = \mu = 200$ GeV, $\tilde{m}_U = \tilde{m}_U^c$, $\tan\beta = 2$,

$m_Q = 500$ GeV and $m_A = 300$ GeV^{*j*}. The solid line represents the leading order result obtained by setting a renormalization scale $Q = m_b$ in the leading order QCD corrections, where m_b is the bottom mass. The dashed line represents the result obtained by setting a normalization scale $Q = 0.5 m_b$, which leads to results in agreement with the most recent next to leading order corrections in the Standard Model⁵⁸. It is clear from the figure that negative values of $\text{Re}(A_t \times \mu)$ are favored to get consistency with the present experimental range⁵⁹, $\text{BR}(b \rightarrow s\gamma)^{\text{exp}} = (2.3 \pm 0.6) \times 10^{-4}$. Since negative values of $\text{Re}(A_t \times \mu)$ imply non-negligible mixing in the stop sector, this rare b-decay imposes very strong constraints on the scenario of electroweak baryogenesis. More information may be obtained by the precise measurement of CP-violating asymmetries at B-factories. Indeed, since the light stop couples via superweak interactions to the bottom sector, the large CP-odd phases associated with this scenario will naturally imply a departure from the Standard Model predictions for these CP-violating asymmetries.

7 CONCLUDING REMARKS

If the scenario of electroweak baryogenesis is realized in nature, it will demand new physics at scales of order of the weak scale. A light Higgs, with mass at the reach of LEP2 will strongly favor this scenario, while new light scalars with relevant couplings to the Higgs field must also be present. These properties are naturally fulfilled within supersymmetric extensions of the Standard Model. The Higgs is naturally light, while the new scalars are provided by the supersymmetric partners of the top quark. Since the stops are charged and colored particles, their large multiplicity helps in enhancing the strength of the first order phase transition, allowing the preservation of the generated baryon number.

The most relevant new CP-violating sources are associated with the supersymmetric partners of the charged and neutral Higgs and weak gauge bosons. These CP-violating sources, which appear through the Higgsino-gaugino mixing terms, must be of order one in order to have a relevant effect in the generation of the baryon asymmetry. Since sizeable phases in the Higgsino mass parameter could lead to unacceptable values for the electric dipole moment of the neutron, one needs to require that the first and second generation squark masses are of the order of a few TeV, or else, an unnatural cancellation between different contributions must take place.

It is interesting to emphasise that the mechanism of electroweak baryogenesis can be consistent with the general framework of unification of couplings.

^{*j*}We have ignored the effect of the CP-violating phases for these computations

In fact, performing a detailed renormalization group analysis, one can match the specific hierarchy of soft supersymmetry breaking terms at low energies required by the electroweak baryogenesis scenario together with large, perturbative values of the top Yukawa coupling, as those associated with the unification of bottom-tau Yukawa couplings or the top quark infrared fixed point structure. A recent study⁵⁴ shows that, depending on the scale at which supersymmetry breakdown is transmitted to the observable sector, the above implies very specific constraints on the stop and Higgs mass parameters of the theory at high energies.

Most important, the electroweak baryogenesis explanation can be explicitly tested at present and near future experiments. In the last phase of LEP2, a center of mass energy $\sqrt{s} \simeq 192$ GeV will be achieved, with a total integrated luminosity of about $100\text{--}150\text{ pb}^{-1}$ per year and per experiment. A lightest CP-even Higgs, with mass of about 100 GeV is expected to be detectable (or otherwise excluded) providing a definite test of the scenario of EWB within the MSSM. The CP-odd mass within this framework must be sufficiently large in order to avoid weakening the first order phase transition, and it must be sufficiently small to avoid the suppression of the new CP-violating sources. Altogether this implies that the lightest Higgs should be quite Standard model like. If the Higgs is found, the next test of this scenario will come from stop searches at a high luminosity Tevatron facility. Moreover, although this is not required, the charginos and neutralinos might be light, at the reach of LEP2.

Another potential experimental test of this model comes from the rate of flavor changing neutral current processes, like $b \rightarrow s\gamma$. We have shown that, if the CP-odd Higgs mass is not sufficiently large, this rate will be in general above the Standard Model predictions, unless $\text{Re}(A_t \times \mu) \lesssim 0$. Hence, rare processes put additional constraints on the allowed parameter space. Moreover, light stops and light charginos, with additional CP-violating phases associated with the μ and A_t parameters, will have a relevant impact on B-physics, which may be testable at B-factories⁶⁰.

In summary, the realization of electroweak baryogenesis will not only provide the answer to one of the most interesting open questions of particle physics, but it will imply a rich phenomenology at present and near future colliders.

Acknowledgements

We would like to thank J.R. Espinosa, A. Riotto, I. Vilja and, in particular, M. Quiros for enjoyable and fruitful collaborations related to this subject. We would also like to thank P. Chankowski, J. Cline, H. Haber, K. Kainulainen,

G. Kane, M. Laine, A. Nelson, M. Pietroni, S. Pokorski and M. Shaposhnikov for many pleasant and interesting discussions.

References

1. G. t'Hooft, *Phys. Rev. Lett.* **37** (1976) 8; *Phys. Rev.* **D14** (1976) 3432.
2. H. Dreiner and G. Ross, *Nucl. Phys.* **B410** (1993) 188.
3. A.D. Sakharov, *JETP Lett.* **91B** (1967) 24.
4. For recent reviews, see: A.G. Cohen, D.B. Kaplan and A.E. Nelson, *Annu. Rev. Nucl. Part. Sci.* **43** (1993) 27; M. Quirós, *Helv. Phys. Acta* **67** (1994) 451; V.A. Rubakov and M.E. Shaposhnikov, *Phys. Usp.* **39** (1996) 461 [hep-ph/9603208].
5. P. Arnold and L. McLerran, *Phys. Rev.* **D36** (1987) 581; and **D37** (1988) 1020; S.Yu Khlebnikov and M.E. Shaposhnikov, *Nucl. Phys.* **B308** (1988) 885; F.R. Klinkhamer and N.S. Manton, *Phys. Rev.* **D30** (1984) 2212; B. Kastening, R.D. Peccei and X. Zhang, *Phys. Lett.* **B266** (1991) 413; L. Carson, Xu Li, L. McLerran and R.-T. Wang, *Phys. Rev.* **D42** (1990) 2127; M. Dine, P. Huet and R. Singleton Jr., *Nucl. Phys.* **B375** (1992) 625.
6. M. Shaposhnikov, *JETP Lett.* **44** (1986) 465; *Nucl. Phys.* **B287** (1987) 757 and **B299** (1988) 797.
7. M.E. Carrington, *Phys. Rev.* **D45** (1992) 2933; M. Dine, R.G. Leigh, P. Huet, A. Linde and D. Linde, *Phys. Lett.* **B283** (1992) 319; *Phys. Rev.* **D46** (1992) 550; P. Arnold, *Phys. Rev.* **D46** (1992) 2628; J.R. Espinosa, M. Quirós and F. Zwirner, *Phys. Lett.* **B314** (1993) 206; W. Buchmüller, Z. Fodor, T. Helbig and D. Walliser, *Ann. Phys.* **234** (1994) 260.
8. J. Bagnasco and M. Dine, *Phys. Lett.* **B303** (1993) 308; P. Arnold and O. Espinosa, *Phys. Rev.* **D47** (1993) 3546; Z. Fodor and A. Hebecker, *Nucl. Phys.* **B432** (1994) 127.
9. W. Buchmüller, Z. Fodor and A. Hebecker, *Nucl. Phys.* **B447** (1995) 131; W. Buchmüller, preprint DESY 96-216 [hep-ph/9610335]
10. K. Kajantie, K. Rummukainen and M.E. Shaposhnikov, *Nucl. Phys.* **B407** (1993) 356; Z. Fodor, J. Hein, K. Jansen, A. Jaster and I. Montvay, *Nucl. Phys.* **B439** (1995) 147; K. Kajantie, M. Laine, K. Rummukainen and M.E. Shaposhnikov, *Nucl. Phys.* **B466** (1996) 189
11. K. Jansen, *Nucl. Phys. (Proc. Supl.)* **B47** (1996) 196.
12. G.R. Farrar and M.E. Shaposhnikov, *Phys. Rev. Lett.* **70** (1993) 2833, (**E**): **71** (1993) 210 and *Phys. Rev.* **D50** (1994) 774.
13. M.B. Gavela, P. Hernández, J. Orloff, O. Pène and C. Quimbay, *Mod. Phys. Lett.* **9** (1994) 795; *Nucl. Phys.* **B430** (1994) 382; P. Huet

- and E. Sather, *Phys. Rev.* **D51** (1995) 379.
14. N. Cabibbo, L. Maiani, G. Parisi and R. Petronzio, *Nucl. Phys.* **B158** (1979) 295; M. Lindner, *Z. Phys.* **C31** (1986) 295; M. Lindner, M. Sher and H.W. Zaglauer, *Phys. Lett.* **B179** (1989) 273; M. Sher *Phys. Lett.* **B317** (1993) 159, *Phys. Lett.* **B331** (1994) 448; C. Ford, D.R.T. Jones, P.W. Stephenson and M.B. Einhorn, *Nucl. Phys.* **B395** (1993) 17
 15. G. Altarelli and I. Isidori, *Phys. Lett.* **B337** (1994) 141.
 16. J.A. Casas, J.R. Espinosa and M. Quiros, *Phys. Lett.* **B342** (1995) 171; *Phys. Lett.* **B382** (1996) 374.
 17. CDF Collaboration, F. Abe *et al.*, *Phys. Rev. Lett.* **74** (1995) 2626; D0 Collaboration, S. Abachi *et al.* *Phys. Rev. Lett.* **74** (1995) 2632; P. Tipton, presented at the XXVIII International Conference on High-Energy Physics, Warsaw, Poland, July 1996.
 18. G.F. Giudice, *Phys. Rev.* **D45** (1992) 3177; S. Myint, *Phys. Lett.* **B287** (1992) 325.
 19. J.R. Espinosa, M. Quirós and F. Zwirner, *Phys. Lett.* **B307** (1993) 106.
 20. A. Brignole, J.R. Espinosa, M. Quirós and F. Zwirner, *Phys. Lett.* **B324** (1994) 181.
 21. M. Carena, M. Quirós and C.E.M. Wagner, *Phys. Lett.* **B380** (1996) 81.
 22. J.R. Espinosa, *Nucl. Phys.* **B475** (1996) 273.
 23. M. Laine, *Nucl. Phys.* **B481** (1996) 43; J. M. Cline, K. Kainulainen, *Nucl. Phys.* **B482** (1996) 73; G.R. Farrar and M. Losada, preprint RU-96-26 [hep-ph/9612346].
 24. D. Delepine, J.M. Gerard, R. Gonzalez Felipe and J. Weyers, *Phys. Lett.* **B386** (1996) 183.
 25. J.M. Moreno, D.H. Oaknin and M. Quirós, to appear in *Nucl. Phys.* **B** [hep-ph/9605387] and preprint IEM-FT-146/96 [hep-ph/9612212].
 26. M. Worah, preprint SLAC-PUB-7417, [hep-ph/9702423]
 27. L. Dolan and R. Jackiw, *Phys. Rev.* **D9** (1974) 3320.
 28. M. Carena, P. Zerwas and the Higgs Physics Working Group, in Vol. 1 of Physics at LEP2, G. Altarelli, T. Sjöstrand and F. Zwirner, eds., Report CERN 96-01, Geneva (1996).
 29. G. Cowan, for the ALEPH collaboration, CERN seminar, Feb. 25th, 1997. <http://alephwww.cern.ch/ALPUB/seminar/Cowan-172-jam/cowan.html>
 30. See, e.g., H. P. Nilles, *Phys. Rep.* **110** (1984) 1; H.E. Haber and G.L. Kane, *Phys. Rep.* **117**(1985) 75.
 31. See, e.g., J.F. Gunion, H.E. Haber, G.L. Kane and S. Dawson, *The Higgs Hunter's Guide*, Addison-Wesley 1990.
 32. Y. Okada, M. Yamaguchi and T. Yanaguida, *Prog. Theor. Phys.* **85**

- (1991) 1; *Phys. Lett.* **B262** (1991) 54; J. Ellis, G. Ridolfi and F. Zwirner, *Phys. Lett.* **B257** (1991) 83; K. Sasaki, M. Carena and C.E.M. Wagner, *Nucl. Phys.* **B381** (1992) 66; H.E. Haber and R. Hempfling, *Phys. Rev. Lett.* **66** (1991) 1815; R. Barbieri, M. Frigeni and F. Caravaglios, *Phys. Lett.* **B258** (1991) 167; H.E. Haber and R. Hempfling, *Phys. Rev.* **D48** (1993) 4280.
33. M. Carena, J.R. Espinosa, M. Quirós and C.E.M. Wagner, *Phys. Lett.* **B355** (1995) 209; M. Carena, M. Quirós and C.E.M. Wagner, *Nucl. Phys.* **B461** (1996) 407; H.E. Haber, R. Hempfling and A.H. Hoang, CERN-TH/95-216, preprint [hep-ph/9609331].
 34. G.W. Anderson and L.J. Hall, *Phys. Rev.* **D45** (1992) 2685.
 35. D. Comelli and J.R. Espinosa, preprint DESY 96-114, FTUV/96-37, IFIC/96-45, IEM-FT-134/96 [hep-ph/9606438].
 36. A.G. Cohen, D.B. Kaplan, and A.E. Nelson, *Phys. Lett.* **B263** (1991) 86.
 37. D. Comelli and M. Pietroni, *Phys. Lett.* **B306** (1993) 67; D. Comelli and M. Pietroni and A. Riotto, *Nucl. Phys.* **B412** (1994) 441; *Phys. Rev.* **D50** (1994) 7703; *Phys. Lett.* **343** (1995) 207; J.R. Espinosa, J.M. Moreno, M. Quirós, *Phys. Lett.* **B319** (1993) 505.
 38. V.A. Kuzmin, V.A. Rubakov and M.E. Shaposhnikov, *Phys. Lett.* **B155** (1985) 36.
 39. M. Carena, M. Quiros, A. Riotto, I. Vilja and C.E.M. Wagner, CERN preprint CERN-TH/96-242, [hep-ph/9702409].
 40. L. Mc Lerran *et al.*, *Phys. Lett.* **B256** (1991) 451; M. Dine, P. Huet and R. Singleton Jr., *Nucl. Phys.* **B375** (1992) 625; M. Dine *et al.*, *Phys. Lett.* **B257** (1991) 351; A.G. Cohen and A.E. Nelson, *Phys. Lett.* **B297** (1992) 111.
 41. D. Comelli, M. Pietroni and A. Riotto, *Phys. Lett.* **B354** (1995) 91 and *Phys. Rev.* **D53** (1996) 4668.
 42. A.G. Cohen, D.B. Kaplan, and A.E. Nelson, *Phys. Lett.* **336** (1994) 41.
 43. M. Joyce, T. Prokopec and N. Turok, *Phys. Rev. Lett.* **75** (1995) 1695, (E): *ibidem* 3375; D. Comelli, M. Pietroni and A. Riotto, *Astropart. Phys.* **4** (1995) 71.
 44. See, for instance: K. Chou, Z. Su, B. Hao and L. Yu, *Phys. Rep.* **118** (1985) 1 and references therein.
 45. N.P. Landsmann and Ch.G. van Weert, *Phys. Rep.* **145** (1987) 141.
 46. A. Riotto, *Phys. Rev.* **D53** (1996) 5834.
 47. P. Huet and A.E. Nelson, *Phys. Lett.* **B355** (1995) 229; *Phys. Rev.* **D53** (1996) 4578.
 48. H.A. Weldon, *Phys. Rev.* **D26** (1982) 1394; V.V. Klimov, *Sov. Phys.*

- JETP* **55** (1982) 199.
49. P.A. Henning, *Phys. Rep.* **253** (1995) 235.
 50. J. Ambjorn and A. Krasnitz, *Phys. Lett.* **B362** (1995) 97.
 51. P. Arnold, D. Son and L.G. Yaffe, preprint UW-PT-96-19 [hep-ph/9609481].
 52. B. de Carlos and J.-R. Espinosa, preprint SUSX-TH-97-005 [hep-ph/9703212].
 53. M. Carena, M. Quiros, A. Riotto and C.E.M. Wagner, in preparation.
 54. M. Carena, P. Chankowski, M. Olechowski, S. Pokorski and C.E.M. Wagner, preprint CERN-TH-96-241, [hep-ph/9612261], to appear in *Nucl. Phys.* **B**.
 55. L. Alvarez Gaumé, J. Polchinski and M.B. Wise, *Nucl. Phys.* **B221** (1983) 495; J. Bagger, S. Dimopoulos and E. Masso, *Phys. Rev. Lett.* **55** (1985) 920; M. Carena, T.E. Clark, C.E.M. Wagner, W.A. Bardeen and K. Sasaki, *Nucl. Phys.* **B369** (1992) 33; N. Polonsky, *Phys. Rev.* **D54** (1996) 4537.
 56. Report of the TeV2000 study Group, FERMILAB-PUB-96/082.
 57. S. Bertolini, F. Borzumati, A. Masiero and G. Ridolfi, *Nucl. Phys.* **B353** (1991) 591; R. Barbieri and G. Giudice, *Phys. Lett.* **B309** (1993) 86.
 58. C. Greub, T. Hurth and D. Wyler, *Phys. Lett.* **B380** (1996) 385; *Phys. Rev.* **D54** (1996) 3350; K. Chetyrkin, M. Misiak and M. Münz, [hep-ph/9612313]; K. Adel and Y.P. Yao, *Phys. Rev.* **D49** (1994) 4945; C. Greub and T. Hurth [hep-ph/9703349].
 59. M.S. Alam et al. (CLEO Collaboration), *Phys. Rev. Lett.* **74** (1995) 2885.
 60. See, for example, A. Cohen, D.B. Kaplan, F. Lepeintre and A.E. Nelson, *Phys. Rev. Lett.* **78** (1997) 2303.